DISCUSSION CONCERNING THE CURRENT CIRCULATION ALONG THE ROMANIAN BLACK SEA COAST

Irina DINU[1], Marco BAJO[2], Giuliano LORENZETTI[2], Georg UMGIESSER[2,3], Luca ZAGGIA[2], Gabriela MAXIMOV[1], Adrian STĂNICĂ[1]

[1]Institute of Marine Geology and Geoecology - GeoEcoMar; 23-25 Dimitrie Onciul St., RO-024053, Bucharest 2, Romania;
e-mail: irinadinu@geoecomar.ro, astanica@geoecomar.ro, gmaximov@geoecomar.ro
[2]Institute of Marine Sciences ISMAR-CNR; Arsenale - Tesa 104, Castello 2737/F, 30122 Venice, Italy;
e-mail: marco.bajo@ve.ismar.cnr.it, giuliano.lorenzetti@ve.ismar.cnr.it, georg.umgiesser@ve.ismar.cnr.it, luca.zaggia@ve.ismar.cnr.it
[3]Coastal Research and Planning Institute, CORPI, Klaipeda University; H. Manto 84, LT 92294, Klaipeda, Lithuania;
e-mail: georg.umgiesser@ve.ismar.cnr.it

Abstract. An integrated approach was used to understand how wind and freshwater input influence the water circulation along the Romanian Black Sea coast. Field data from different ADCP (Acoustic Doppler Current Profiler) surveys in the area of the delta were combined with a 3D finite element model. The model SHYFEM (Shallow Water HYdrodynamic Finite Element Model), developed at the Institute of Marine Sciences (ISMAR – National Research Council, Venice, Italy), was used on the entire Black Sea, with higher resolution near the Romanian coast and the Danube River distributaries. Several theoretical simulations were carried out, varying the wind velocity and river discharge, according to the available long-term data and using measured data as a reference for model validation. The simulated currents have the same order of magnitude as the measured ones.

The results show that the Danube discharge influences the circulation along the entire Romanian Black Sea coast, generating a longshore current, mainly localized in the surface layers. This current occurs even at low river discharges and is found both at low and high wind velocity. In this study we compared the results of the simulations for two main wind directions, NE and SE, but the wind from SW (generally inland) was also considered since it is opposite to the downdrift buoyant flow propagation. Maps of the current field and the fluxes, calculated on several sections perpendicular to the coast, were analyzed for all these forcings. We made the simulations both for the cold and warm season, by applying different temperature and salinity fields.

The results show that, for both cold and warm seasons, the constantly blowing wind becomes a significant factor in the formation of coastal currents.

Calculated fluxes on cross-sections versus Danube discharge usually show important differences between the cold and warm seasons, which are due to the distribution of temperature and salinity. Those seasonal differences are less significant in the case of increased wind velocity. Thus, at higher velocity, wind becomes a dominant factor, controlling the overall circulation.

This study is a first step towards the development of a fully operational oceanographic model for the northwestern part of the Black Sea. Future developments will include the use of real meteorological forcing, modelling of the waves and sediment transport.

Key words: current direction and velocity, 3D hydrodynamic model, theoretical simulation, wind direction and velocity, Danube discharge

1. INTRODUCTION

Complex processes occur at river mouths and in surrounding areas, due to the interaction between the freshwater inputs from the rivers and the mixing with seawater. These interactions strongly influence the general coastal and marine circulation over extensive areas. The coastal circulation at river mouths is even more complicated by the significant forcing represented by wind regime and its variations.

The Romanian Black Sea coastal dynamics is strongly influenced by the buoyant flow of the Danube water. The Romanian coastline is divided into two units, separated by Cape Midia, which represents a physical separation in the general

southerly sediment transport, due to the presence of the Midia Harbor jetties (Fig. 1). These are 5 km long structures which interrupt the longshore drift of sediments originating from the Danube river and transported southward, as mentioned by Spătaru (1990), Panin (1998), Giosan *et al*. (1999), Ungureanu and Stănică (2000). In the southern unit of the Romanian coast, the current pathways are influenced mainly by natural coastal morphology, coastal structures and harbor defense works. The effects of the Danube inputs of water and alluvia on the northwestern Black Sea coast were analyzed, among others, by Panin and Jipa (2002). The dynamics of the coastal sediments in front of the Danube Delta and ways in which humans have induced perturbances in the natural coastal evolution have been analyzed by several research groups, among whom Panin (1998), Giosan *et al*. (1999), Ungureanu and Stănică (2000), Stănică *et al*. (2007; 2011), Vespremeanu-Stroe *et al*. (2007) and Dan *et al*. (2007; 2009).

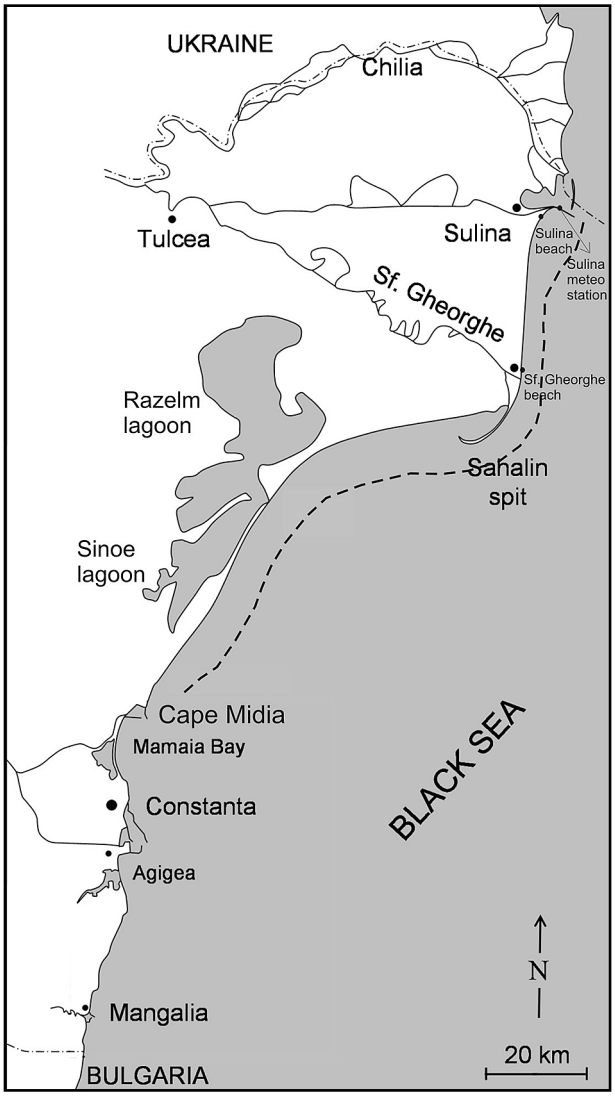

Fig 1. Sketch of the Romanian coast. *Note:* the dotted line marks the extension of the ADCP profiles.

A detailed study concerning the influence of the shelf-break forcing on the Danube buoyant water along the western coast of the Black Sea, based on two surveys conducted in the July 1992 and May 1994, was performed by Yankovsky *et al*. (2004). The buoyant water exhibited different downstream penetration, influenced by anticyclones and mesoscale eddies associated with the Rim Current. The influence of downwelling-favourable or upwelling-favourable wind on the current circulation is also discussed within this study.

The general Black Sea circulation was previously studied using numerical modelling. We can mention the works performed by Oguz and Malanotte-Rizzoli (1996), using the Princeton Ocean Model (POM), by Stanev and Beckers (1999a, b) and Beckers *et al*. (2002), using the GeoHydrodynamics and Environment Research (GHER 3D) model, by Staneva *et al*. (2001), using the Dietrich Center for Air Sea Technology (DieCAST) model, by Stanev *et al*. (2003), using the Black Sea Modular Ocean Model (MOM) and by Kara *et al*. (2005; 2008), using the Hybrid Coordinate Ocean Model (HYCOM). An overview of the numerical modelling used to simulate circulation and transport of matter in the Black Sea was performed by Stanev (2005).

The purpose of this study is to investigate the influence of wind and Danube river discharge on the formation and characteristics of the coastal currents along the Romanian Black Sea coast. Waves were not included in the hydrodynamic model at this stage of the study. The influence of the Danube water flow on the northwestern part of the Black Sea is of particular importance, due to the changing sediment transport capacity of the longshore currents, with direct consequences on the coastal erosion processes, as discussed by Panin and Jipa (2002), Panin (2005), Stănică *et al*. (2007; 2011).

In this study the 3D hydrodynamic model SHYFEM (Shallow Water HYdrodynamic Finite Element Model) was implemented over the entire Black Sea. The model, which was developed at the Institute for Marine Sciences ISMAR-CNR, in Venice, by Umgiesser *et al*. (2004), is the first numerical model used for a detailed investigation on the hydrodynamics along the Romanian Black Sea coast. It was first used in this zone by Tescari *et al*. (2006, focusing on the delta coast between the mouths of Sulina (middle Danube distributary) and Sf. Gheorghe (southern Danube distributary).

According to data from the Romanian National Administration for Meteorology, the most frequent winds on the Romanian Black Sea coast are from NE and SE, as discussed by Bondar *et al*. (1973), Bondar and Panin (2001), Bondar (2006). Moreover, the wind from NE can cause downwelling and can determine the SW propagation of the Danube buoyant flow. The wind from SW is also important, as it may reach velocities over 28 $m \cdot s^{-1}$, as stated by Bondar *et al*. (1973), while it may arrest the penetration of buoyancy-driven coastal currents, as discussed by Yankovsky *et al*. (2004).

Even if this paper mainly discuss theoretical simulations, the current fields provided by the model agree, both in mag-

nitude and direction, with experimental data obtained in similar meteorological conditions, provided by Bondar *et al*. (1973), and Bondar (2006). In June 2011 we performed current measurements on the Romanian coast of the Danube Delta, between Sulina and Cape Midia. Velocities of over 40 $cm \cdot s^{-1}$ were found even at 15 m water depth. The current directions showed high variability, at a depth of around 3 m, most of them being in the S – NW sector, but also N – NE components were reported. For depths higher than 7 m, the current directions were oriented mainly towards the south, but also N – NE components occurred.

At this stage of the study we can preliminarily compare the order of magnitude of the simulated currents in rather similar conditions, for the warm season and low wind velocity. The simulations show as the currents velocity can reach 40 – 50 $cm \cdot s^{-1}$, both in surface and in deeper layers, when the wind is parallel to the coast. Such fast currents are actually found in front of the Danube distributaries, even in the absence of wind, suggesting that they are mainly due to the baroclinic action of the Danube. The model shows that high wind velocities may lead to strong currents, down to a depth of 20 – 30 m, on extended areas of the southern Romanian Black Sea coast. The currents predicted by the model are comparable with the measured ones, with almost similar forcing.

2. METHODS

2.1. Data

2.1.1. Coastline and bathymetry

The Romanian coastline and the bathymetry near the Romanian coast were provided by GeoEcoMar, that has performed many field campaigns on the Romanian Black Sea coast over the years.

For the rest of the Black Sea, we used a coarser coastline of the Black Sea, provided by NOAA (http://rimmer.ngdc.noaa.gov/mgg/coast/getcoast.html), and a coastline extracted from web resources (http://earth.google.com/).

The bathymetry of the other parts of the Black Sea was obtained from the NOAA free on-line service (http://www.ngdc.noaa.gov/mgg/gdas/gd_designagrid.html.

2.1.2. Historical measurements

Current measurements on the Romanian Black Sea coast have been performed over the years in three points: Sulina meteorological station, that is located in a rather sheltered zone, at the beginning of the Sulina jetty (Fig. 1), Sulina beach and Sf. Gheorghe beach. These data were provided by Bondar *et al*. (1973), Bondar (2006).

2.1.3. New current survey

Currents were measured in May and June 2011 on the Romanian Black Sea coast between Sulina and Cape Midia, a coastal sector about 120 km long. A total number of 42 transects perpendicular to the coastline were acquired with a boat mounted Acoustic Doppler Current Profiler (ADCP). The instrument used was a 600 kHz a Workhorse Rio Grande ADCP (Teledyne-RDI, USA), set to work with a 0.5 m depth cell in mode 12. Each transect starts from the depth of about 2 m and stops at the depth of 15 m. A few transects were also acquired within the river in sections located at approximately 3.5 km from the mouth, near the town of Sf. Gheorghe.

2.2. The model

SHYFEM (Shallow water HYdrodynamic Finite Element Model), described by Umgiesser *et al*. (2004), has been developed at the Institute of Marine Sciences, National Research Council in Venice, and it is based on the method of the finite elements to solve the hydrodynamic equations in lagoons, coastal seas, estuaries and lakes. The model solves the 3D hydrodynamic equations for several water layers, providing a 3D representation of the basin. SHYFEM was applied in several cases around Europe, on lagoons and lakes, as in Ferrarin and Umgiesser (2005), Bellafiore *et al*. (2008), Ferrarin *et al*. (2008), De Pascalis *et al*. (2009), Ghezzo *et al*. (2010), and also in operational oceanography, by Bajo and Umgiesser (2010). SHYFEM was already used on the Romanian Black Sea coast by Tescari *et al*. (2006), focusing on the zone in front of the Danube Delta.

The model uses a staggered grid, defined by nodes and triangular elements, and a semi-implicit algorithm for the integration in time. The staggered grid formulation is necessary to achieve mass conservation. The water level is computed at the nodes, while the velocities are computed at the element centers, using a step shape function. The bathymetry is specified in each element.

The water column is divided into several layers, the first being the surface layer, while the last is the bottom layer. The layer thicknesses are set by the user and are constant, except for the surface layer, which involves the variation due to the water level ζ.

The primitive equations are:

$$\frac{dU_l}{dt} - fV_l + h_l\left[g\frac{\partial\zeta}{\partial x} + \frac{g}{\rho_0}\frac{\partial}{\partial x}\int_{-h_l}^{\zeta}\rho' dz + \frac{1}{\rho_0}\frac{\partial p_a}{\partial x}\right] - \frac{1}{\rho_0}\left(\tau_x^{l-1} - \tau_x^{l}\right) - A_H\Delta U_l = 0$$

$$\frac{dV_l}{dt} + fU_l + h_l\left[g\frac{\partial\zeta}{\partial y} + \frac{g}{\rho_0}\frac{\partial}{\partial y}\int_{-h_l}^{\zeta}\rho' dz + \frac{1}{\rho_0}\frac{\partial p_a}{\partial y}\right] - \frac{1}{\rho_0}\left(\tau_y^{l-1} - \tau_y^{l}\right) - A_H\Delta V_l = 0$$

$$\frac{\partial\zeta}{\partial t} + \sum_l\frac{\partial U_l}{\partial x} + \sum_l\frac{\partial V_l}{\partial y} = 0$$

where ζ is the water level [L], $U_l = h_l u_l$ and $V_l = h_l v_l$ are the vertically-integrated velocities (total transports) for layer l [L^2T^{-1}] and t is the time [T]; g is the gravity acceleration [LT^{-2}], p is the atmospheric pressure at the mean sea level [$ML^{-1}T^{-2}$]; ρ_0 is the undisturbed water density [ML^{-3}]; ρ' is the water density [ML^{-3}]; p_a is the air pressure; h_l is the thickness of the layer l [L]; f is the variable Coriolis parameter [T^{-1}]; τ_x^l and τ_y^l, τ_x^{l-1} and τ_y^{l-1} are the stress components at the lower interface of the layers l and l-1 [$ML^{-1}T^{-2}$]; A_H is the horizontal diffusion parameter [L^2T^{-1}].

On the uppermost layer the wind stress components (τ_x^s and τ_y^s [$ML^{-1}T^{-2}$]) are specified using the formulation by Smith and Banke (1975):

$$\tau_x^s = c_D \rho_a w_x \sqrt{w_x^2 + w_y^2} \quad \text{and} \quad \tau_y^s = c_D \rho_a w_y \sqrt{w_x^2 + w_y^2}$$

where ρ_a is the air density (1.225 kg/m^3), c_D is a dimensionless drag coefficient, varying between 1.5×10^{-3} and 3.2×10^{-3}, and w_x, w_y are the components of the wind velocity in the x and y directions.

On the lowermost layer, the bottom stress components (τ_x^b and τ_y^b [$ML^{-1}T^{-2}$]) are specified as following:

$$\tau_x^b = c_B \rho_0 u_L \sqrt{u_L^2 + v_L^2} \quad \text{and} \quad \tau_y^b = c_B \rho_0 v_L \sqrt{u_L^2 + v_L^2}$$

where c_B is the dimensionless bottom friction coefficient and u_L, v_L [LT^{-1}] are the velocity components in the last layer.

A turbulence closure scheme was used in order to compute the vertical diffusivity. This scheme is an adaptation of the k-ε module of the General Ocean Turbulence Model (GOTM), described by Burchard and Petersen (1999). The horizontal turbulent viscosity has been computed using the model proposed by Smagorinsky (1963).

2.3. Model setup

In the present study the model was implemented on the entire Black Sea and is focused on the Romanian coast, with a gradually increasing resolution towards the shoreline. It uses a staggered grid, defined by 11668 nodes and 21667 triangular elements (Fig. 2).

The grid resolution varies from about 20 km in the central part of the Black Sea to about 100 m near the Romanian coast. This resolution can be considered sufficient to resolve coastal currents due to meteorological forcing and freshwater discharge.

The model comprises 27 layers. The first 10 m of the water column are represented by 2 m thick layers, below this the layer thickness increasing progressively with depth. The last layer of the model is 500 m thick and covers only a restricted area in the centre of the Black Sea.

Open boundary conditions are specified at the Bosphorus Strait and for the main rivers. On the Bosphorus Strait the level is set to zero and the normal fluxes are left free to adjust. The main river inputs considered are: the Danube with its distributaries: Chilia (that forms a secondary delta with four main branches – on the Ukrainian territory), Sulina and Sf. Gheorghe, in Romania; Dnepr, Dnestr and South Bug, in Ukraine.

The distributaries of the Danube are partially represented in the grid, in order to set up the river momentum when it discharges into the Black Sea. The freshwater inputs are spread among the border elements. Discharge is prescribed and horizontal velocities are computed by the model.

The water discharge for the Danube distributaries was introduced taking into account the percentages provided by Panin (2003): Chilia 58%, Sulina 19% and Sfântu Gheorghe 23%. Other discharge values were introduced in the model for the rivers Dnepr, Dnestr and South Bug, on the territory of Ukraine, and were found in Yankovsky *et al*. (2004).

2.4. Simulations

Several hydrodynamic simulations were made using differing initial conditions for the sea state during cold and warm seasons. The maximum time step for the simulations was set to 150 s. The model allows automatic sub-stepping over time, for numerical stability.

Constant wind blowing from various directions, with low and high velocity and different values of Danube discharge

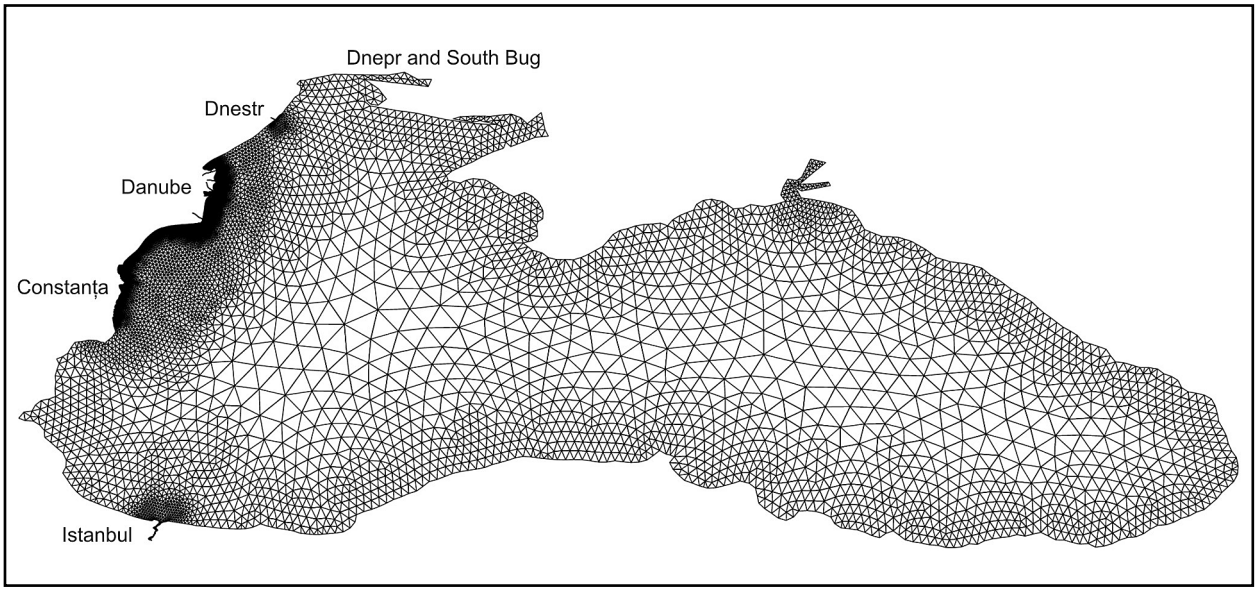

Fig 2. Computational grid of the Black Sea utilized for modelling of the current circulation.

were used. The resulting current maps and fluxes calculated on several cross-sections were compared for all the simulations.

Simulations were performed with constant wind forcing of 5 and 10 $m \cdot s^{-1}$, according to the available data from the Romanian National Meteorological Administration, provided by Bondar (2006). The wind is considered at 10 m height.

For the total Danube discharge, the average value of 6500 $m^3 \cdot s^{-1}$ was used, taken from Panin and Jipa (2002). The discharge for the rivers Dnepr, Dnestr and South Bug were 1000, 400 and 500 $m^3 \cdot s^{-1}$, respectively, provided by Yankovsky *et al*. (2004). Other simulations were made imposing low and high Danube discharge values of 4000 $m^3 \cdot s^{-1}$ and, respectively, 9000 $m^3 \cdot s^{-1}$, according to the available data from Bondar *et al*. (1991). The discharges of the rivers Dnepr, Dnestr and South Bug were modified as well, in order to agree with the change of the total Danube discharge. These discharges are presented in Table 1. For simplification, the Chilia distributaries were numbered from north to south. Therefore, Chilia 1 corresponds to Prorva, Chilia 2 to Oceakovsky, Chilia 3 to Bystroe and Chilia 4 to Stari Stambul.

Initial temperature and salinity conditions for the cold and warm seasons were available from the Mediterranean Data Archiving and Rescue (MEDAR) project (http://medar.ieo.es). This database provides monthly average fields of temperature and salinity for the Mediterranean and the Black Sea, obtained from processed observations. In our study we considered two different initial states, given by the temperature and salinity distributions for January and May, to obtain results for the middle of the cold season, but also for the beginning of the warm season, as previously investigated by Yankovsky *et al*., 2004, in the conditions of high Danube discharge, in May 1994.

The nudging technique used in this work is a relaxation of the modelled temperature and salinity to the observations. The MEDAR fields from January and May are interpolated in the nodes of the Black Sea grid and their differences with the model values are computed. Nudging forcing terms proportional to these differences are added to the model equations. Their weights can be different on each node (and also on each vertical layer) and are called relaxation times. Relaxation times are short (about 1 hour) in the open sea, where the spin-up time is high and requires a strong temperature and salinity forcing. Meanwhile, they are longer near the Romanian coast (about 3 days), where the freshwater forcing is rather strong and spin-up time is shorter.

The analysis presented in this paper was carried out comparing the results of the simulations performed for both cold and warm seasons, under the conditions listed in Table 2.

Seven cross-sections, extending on about 25 km seaward (Fig. 3), were chosen for the comparison of the fluxes calculated for each simulation. The cross-sections extend to a water depth between 35 m for the northernmost section and 175 m for the southernmost one. The first cross-section is located south of the Sulina mouth; the second is located south of Sf. Gheorghe mouth; the third and fourth cross-sections are located, from north to south, in the Perişor area and in front of the barrier beach separating the Razelm and Sinoe lagoons; the fifth cross-section is located north of Midia Harbor, while the sixth is north of the Mangalia town; the last cross-section is located on the Bulgarian coast, close to Cape Kaliakra.

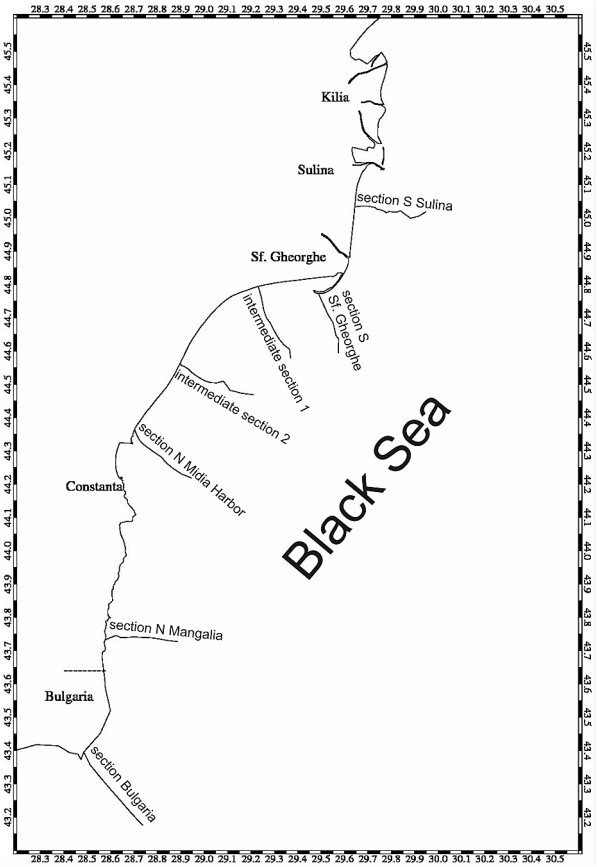

Fig 3. Location of the cross-sections used in the analysis of the wind and freshwater input influence on the coastal currents circulation.

Both for cold and warm season conditions, the first simulations, without wind, were carried out over a 45 days period, for low, medium and high discharge. The simulations with wind forcing were carried out for four days, using the initial state provided by the simulations without wind, given by the distribution of temperature and salinity, in order to reduce the spin-up time of the system.

For every simulation, results are exposed through current maps in the surface layer (which is current at 1 m depth), currents maps at a depth of 9 m, and 2 cross-sections, south of Sulina distributary and north of Mangalia (Figs. 4 – 10). The velocity vectors in the cross-sections are interpolated to the nodes from their element values. Salinity cross-sections in various conditions are also shown (Figs. 11 and 12).

Table 1. Water discharge distribution on the main rivers (Chilia 1-4 are numbered from north to south).

Name	Low discharge ($m^3 \cdot s^{-1}$)	Medium discharge ($m^3 \cdot s^{-1}$)	High discharge ($m^3 \cdot s^{-1}$)
Chilia 1	400	650	900
Chilia 2	800	1300	1800
Chilia 3	480	780	1080
Chilia 4	640	1040	1440
Sulina	760	1235	1710
Sf. Gheorghe	920	1495	2070
Total Danube	*4000*	*6500*	*9000*
Dnepr	600	1000	1400
Dnestr	200	400	500
South Bug	300	500	700

Table 2. Simulation forcings for cold and warm seasons.

Simulation no.	Wind direction	Wind velocity ($m \cdot s^{-1}$)	Total Danube discharge ($m^3 \cdot s^{-1}$)
1	calm (no wind)	-	6500
2	from NE	5	4000
3		10	9000
4	from SE	5	4000
5		10	9000
6	from SW	5	4000
7		10	9000

3. RESULTS

3.1. Model results versus historical data

The magnitude of the current velocity and direction provided by the simulations performed were compared with the available historical data.

Table 3 presents the measured current velocities and directions in these points, as well as the ones provided by the model under similar meteorological conditions, both for the cold and warm seasons. One can notice that the historical data generally agree with the results of the simulations, in terms of magnitude and direction. However, we have no information concerning the Danube discharge at the time of "historical" measurements. This is probably the reason why, for low south-easterly wind in the zone of Sf. Gheorghe beach, the currents provided by the model are lower than the measured ones. The same happens in this sector for low southwesterly wind in warm season. In the simulation, the total Danube discharge associated with low wind velocity was 4000 $m^3 \cdot s^{-1}$ but, more probably, the true discharge was higher.

3.2. Comparison with ADCP measurements from the 2011 field campaigns

The dotted line in Fig. 1 marks the approximate extension of the ADCP profiles, which is between 5 and 10 km offshore. Most of the measured current velocities are between 10 and 30 $cm \cdot s^{-1}$, but also values over 40 $cm \cdot s^{-1}$ have been determined, even at a depth of 15 m. Some profiles were located in the sector where the Sulina jetties induce the formation of medium-scale eddies. Therefore, the variability of the current directions is high.

The discharges measured in the Sf. Gheorghe distributary were around 1500 $m^3 \cdot s^{-1}$. Considering the distribution provided by Panin (2003), we can reasonably infer that the total Danube discharge was around the average value of 6500 $m^3 \cdot s^{-1}$.

Wind data for the period of field measurements were obtained from information available on the site www.vremea.acasa.ro and are provided by the National Meteorological Administration. The surface currents observed in the area are formed by the action of wind occurring from some hours to even one day before.

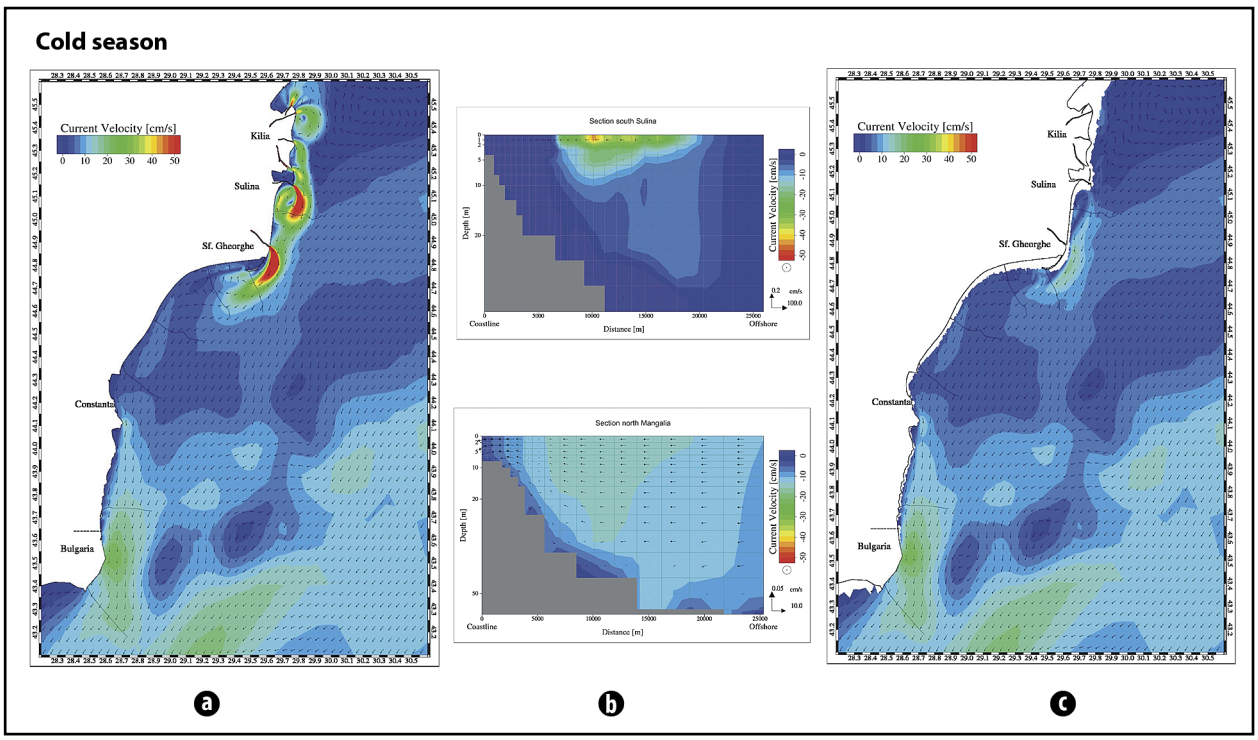

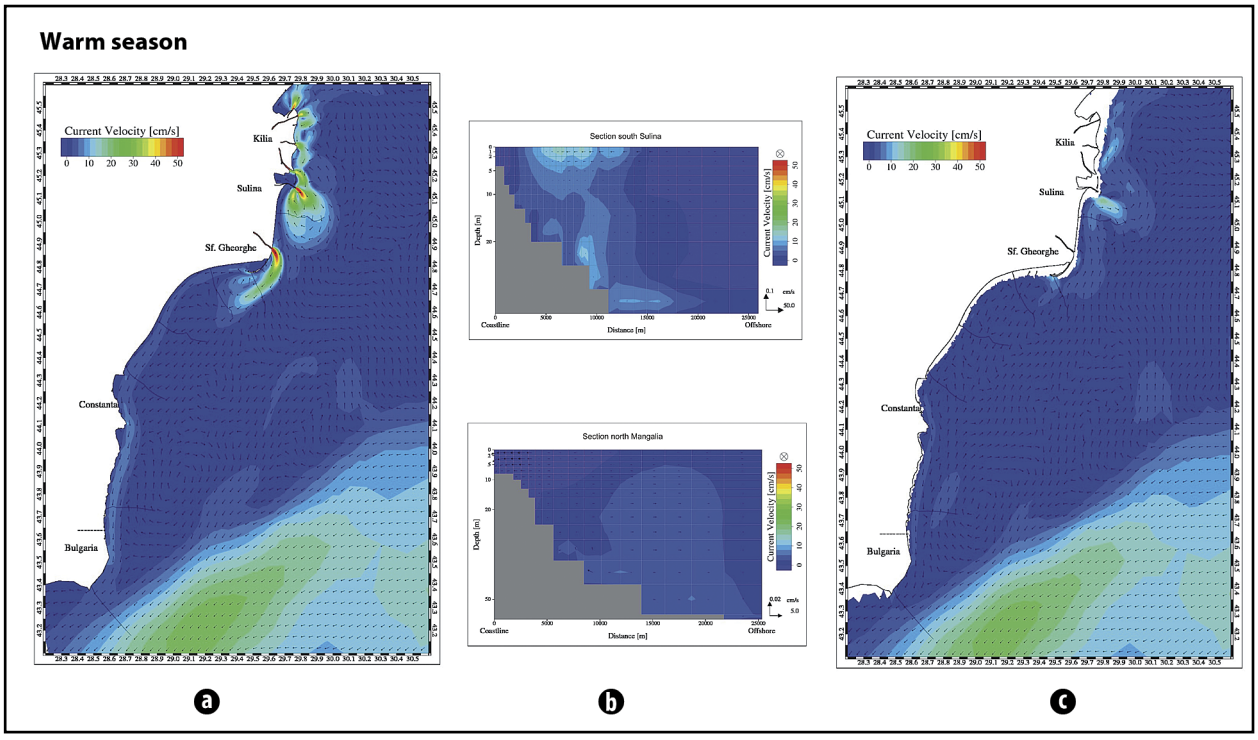

Fig 4. Current patterns along the Romanian Black Sea coast during the cold (upper panel) and warm seasons (lower panel): **a)** map of surficial currents; **b)** currents in the cross-sections located S of Sulina and N of Mangalia; **c)** map of currents at a depth of 9 m – no wind, medium Danube river discharge.

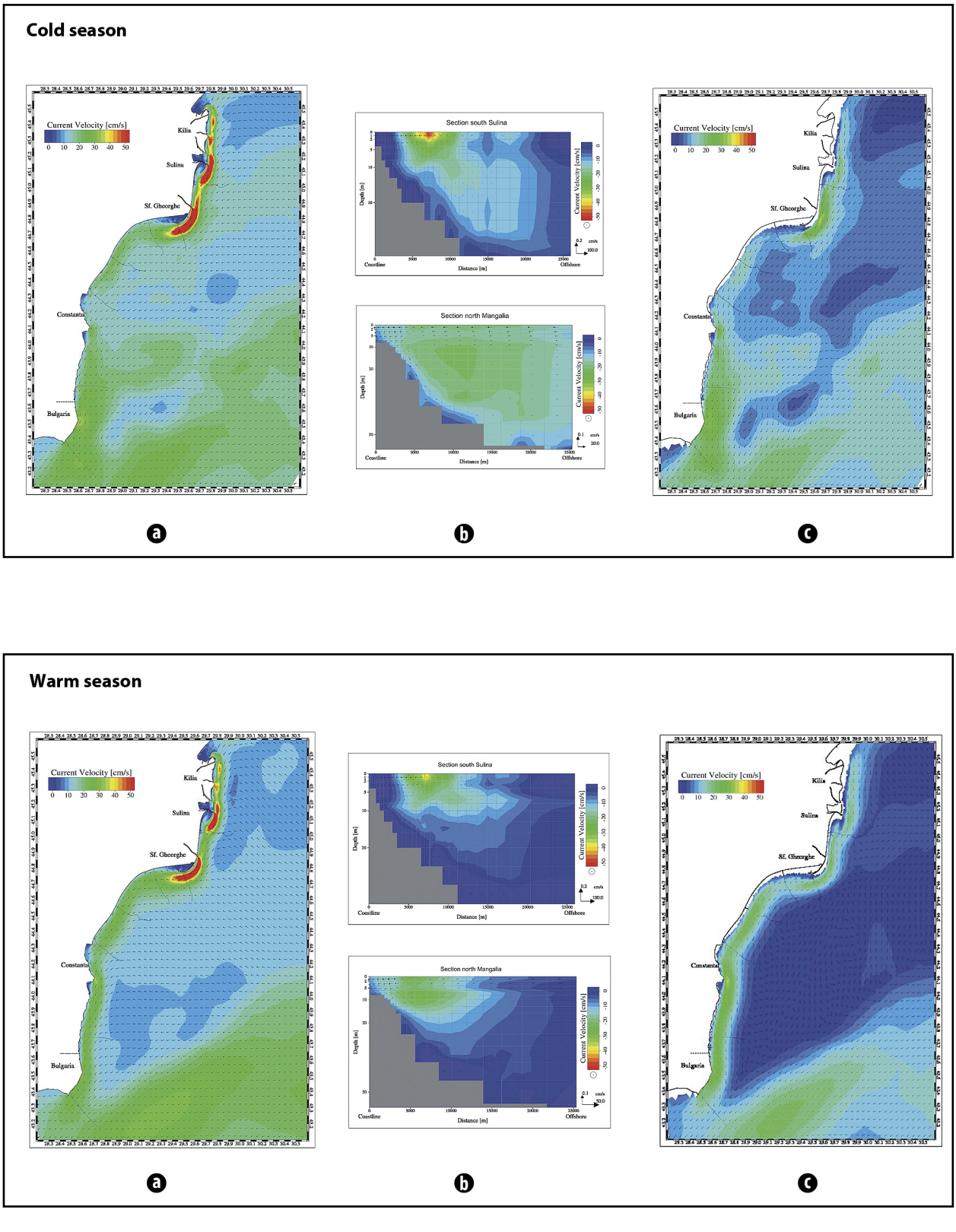

Fig 5. Current patterns along the Romanian Black Sea coast during the cold (upper panel) and warm seasons (lower panel): **a)** map of surficial currents; **b)** currents in the cross-sections located S of Sulina and N of Mangalia; **c)** map of currents at a depth of 9 m – wind from NE with 5 m·s^{-1}, low Danube discharge.

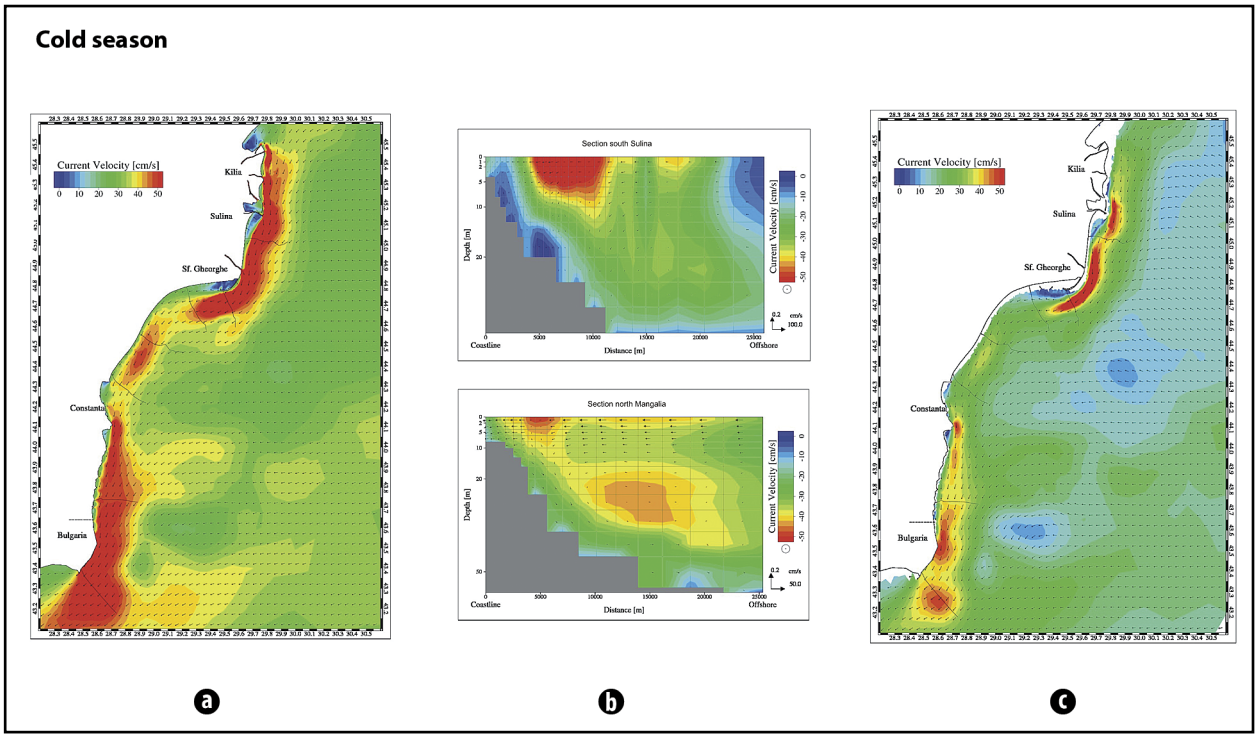

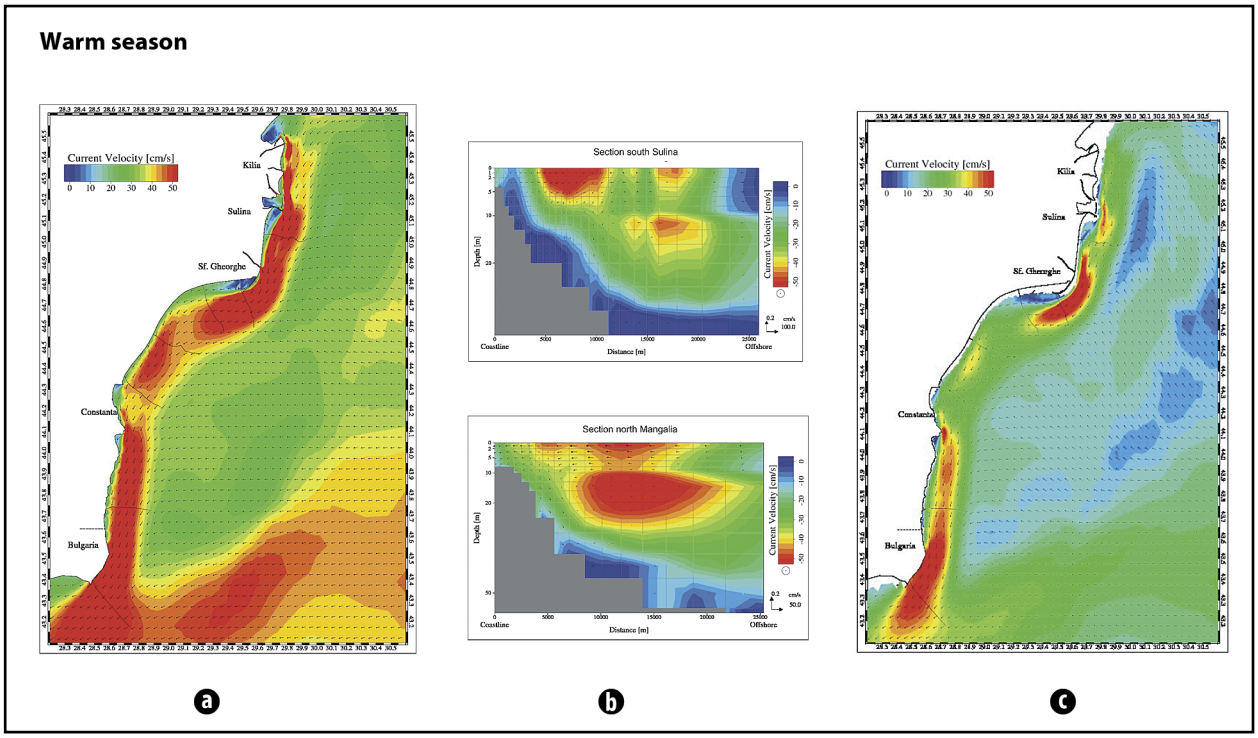

Fig 6. Current patterns along the Romanian Black Sea coast during the cold (upper panel) and warm seasons (lower panel): **a)** map of surficial currents; **b)** currents in the cross-sections located S of Sulina and N of Mangalia; **c)** map of currents at a depth of 9 m – wind from NE with 10 $m \cdot s^{-1}$, high Danube discharge.

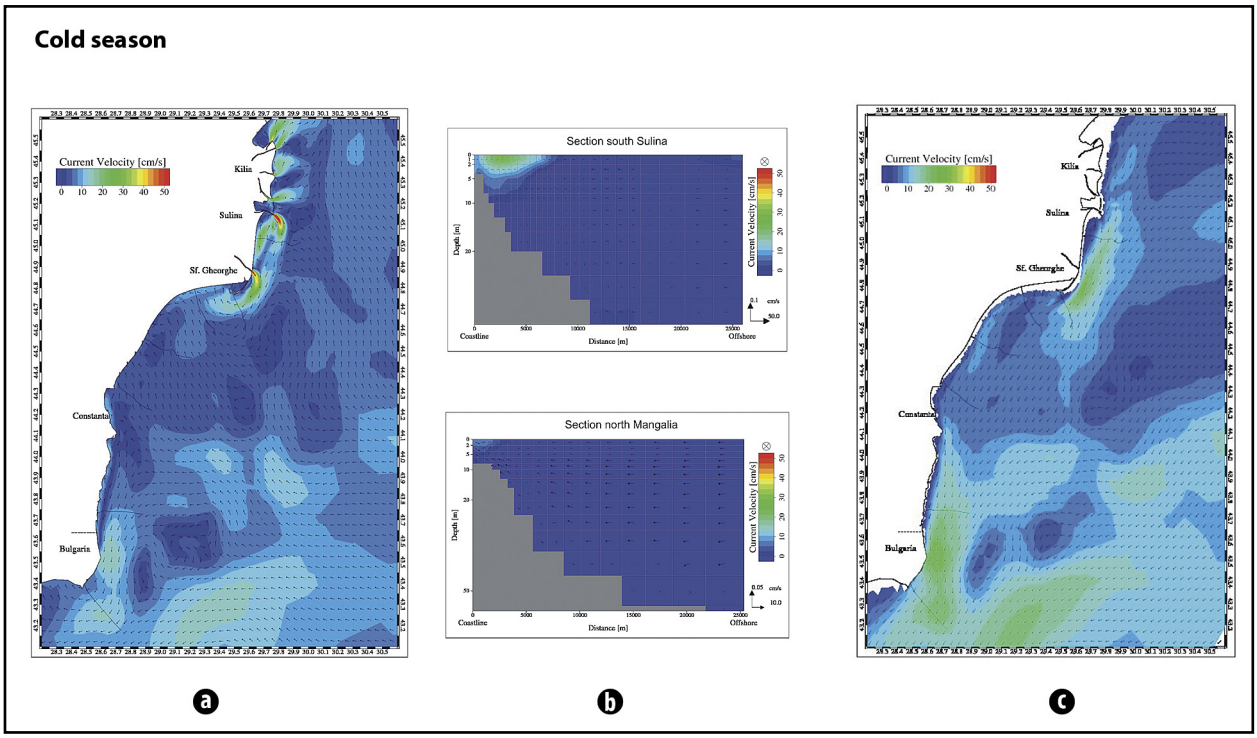

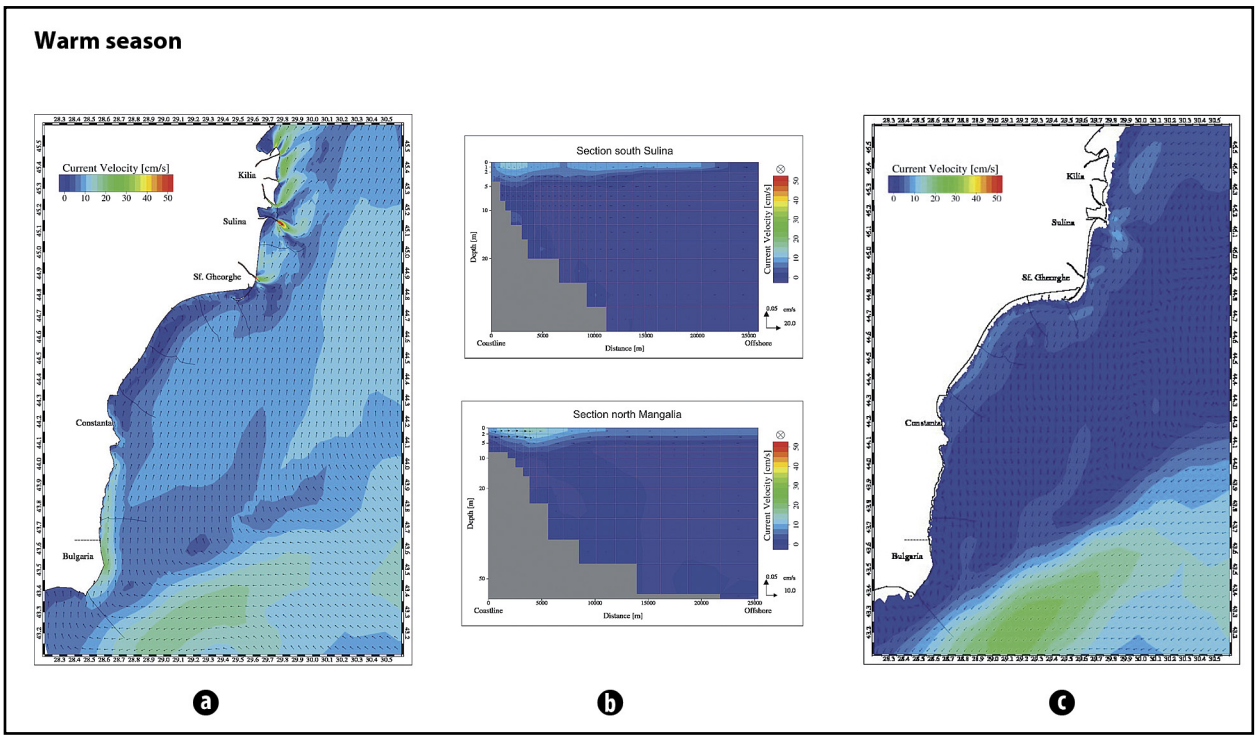

Fig 7. Current patterns along the Romanian Black Sea coast during the cold (upper panel) and warm seasons (lower panel): **a)** map of surficial currents; **b)** currents in the cross-sections located S of Sulina and N of Mangalia; **c)** map of currents at a depth of 9 m – wind from SE with 5 m·s^{-1}, low Danube discharge.

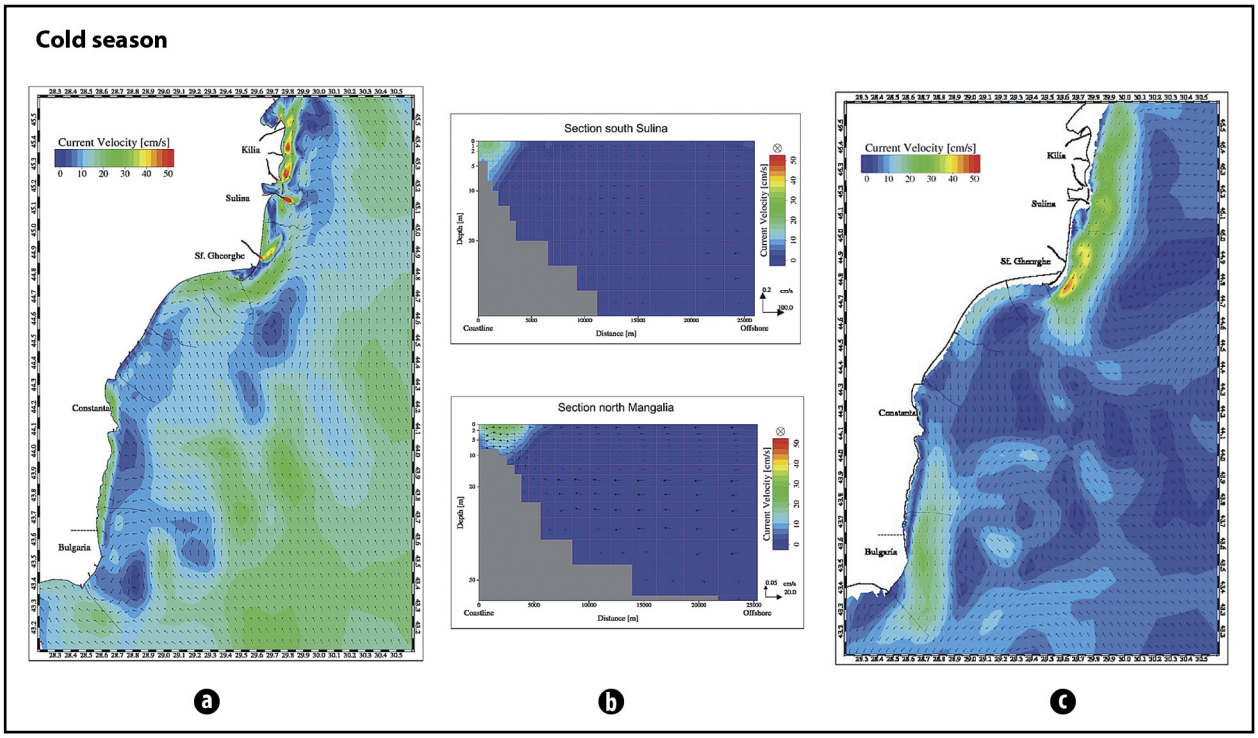

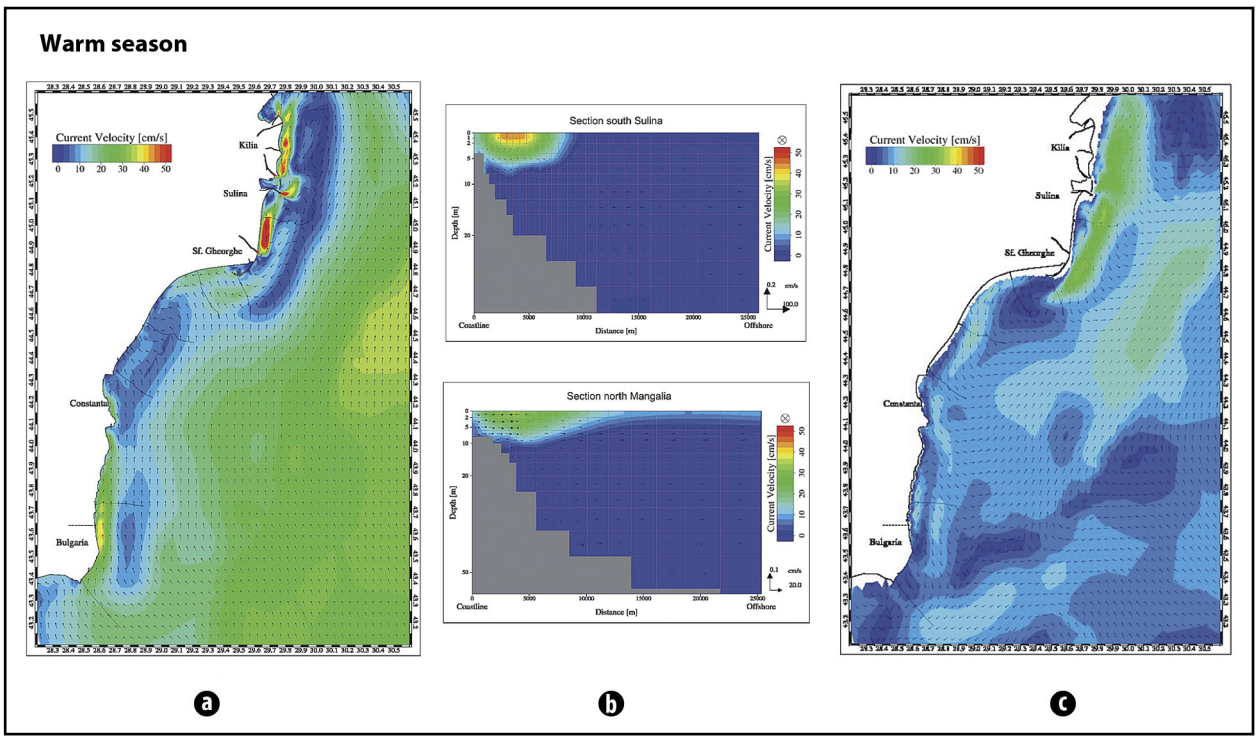

Fig 8. Current patterns along the Romanian Black Sea coast during the cold (upper panel) and warm seasons (lower panel): **a)** map of surficial currents; **b)** currents in the cross-sections located S of Sulina and N of Mangalia; **c)** map of currents at a depth of 9 m – wind from SE with 10 m·s^{-1}, high Danube discharge.

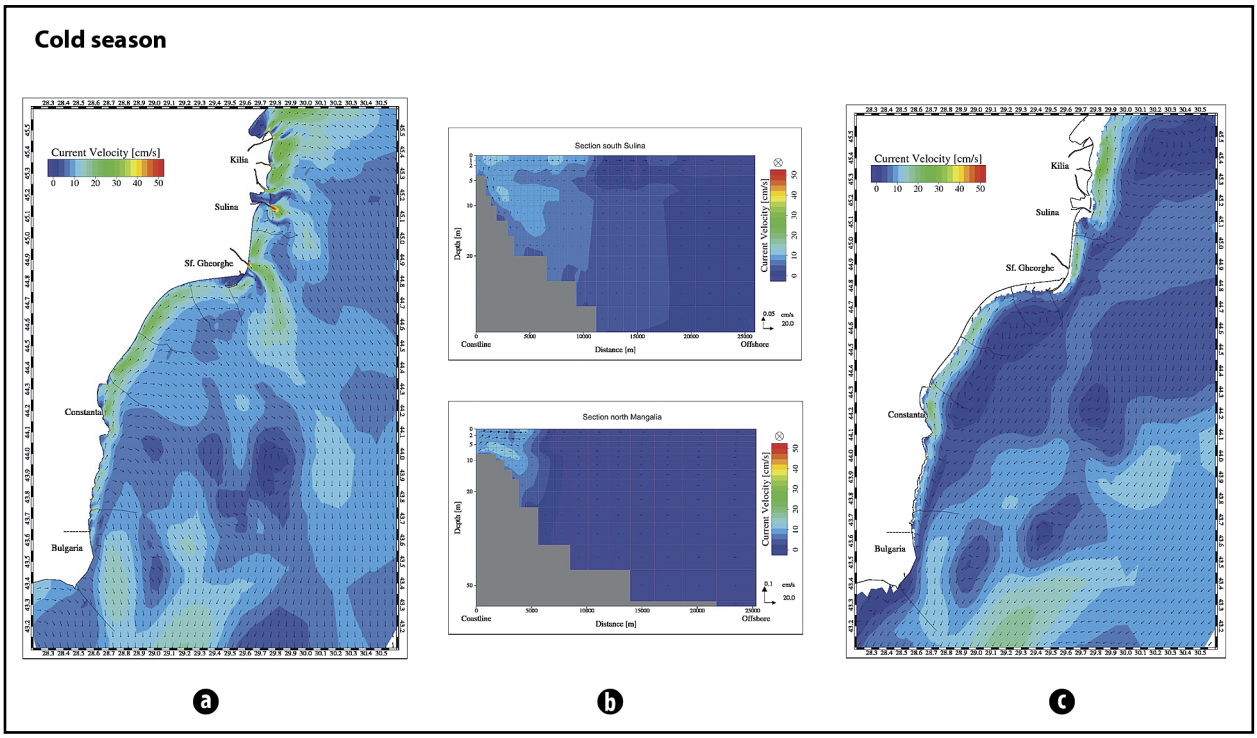

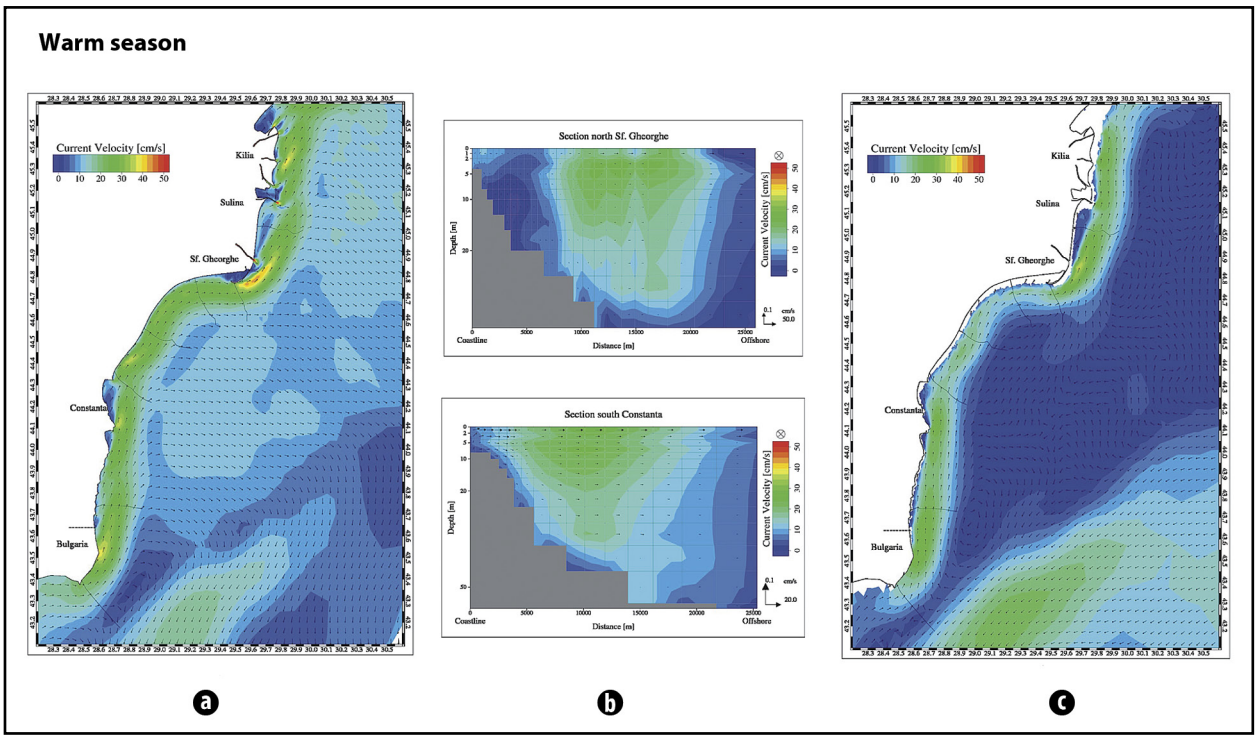

Fig 9. Current patterns along the Romanian Black Sea coast during the cold (upper panel) and warm seasons (lower panel): **a)** map of surficial currents; **b)** currents in the cross-sections located S of Sulina and N of Mangalia; **c)** map of currents at a depth of 9 m – wind from SW with 5 m·s^{-1}, low Danube discharge.

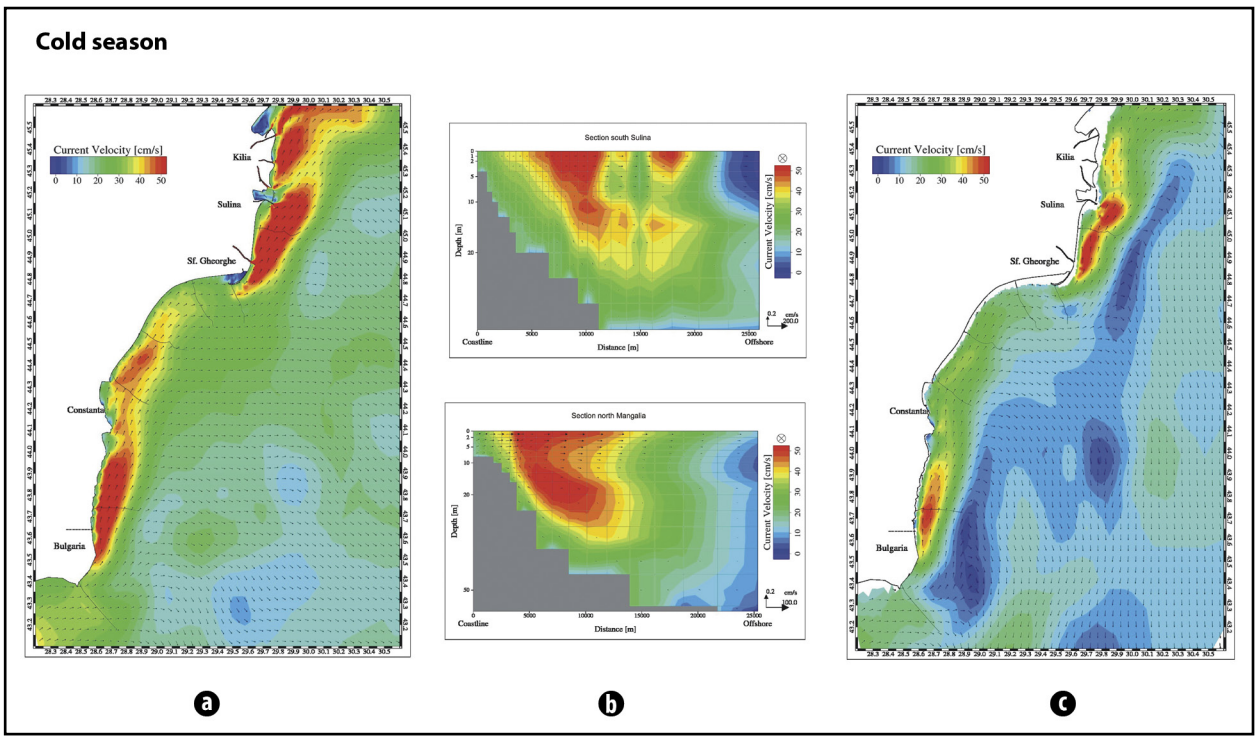

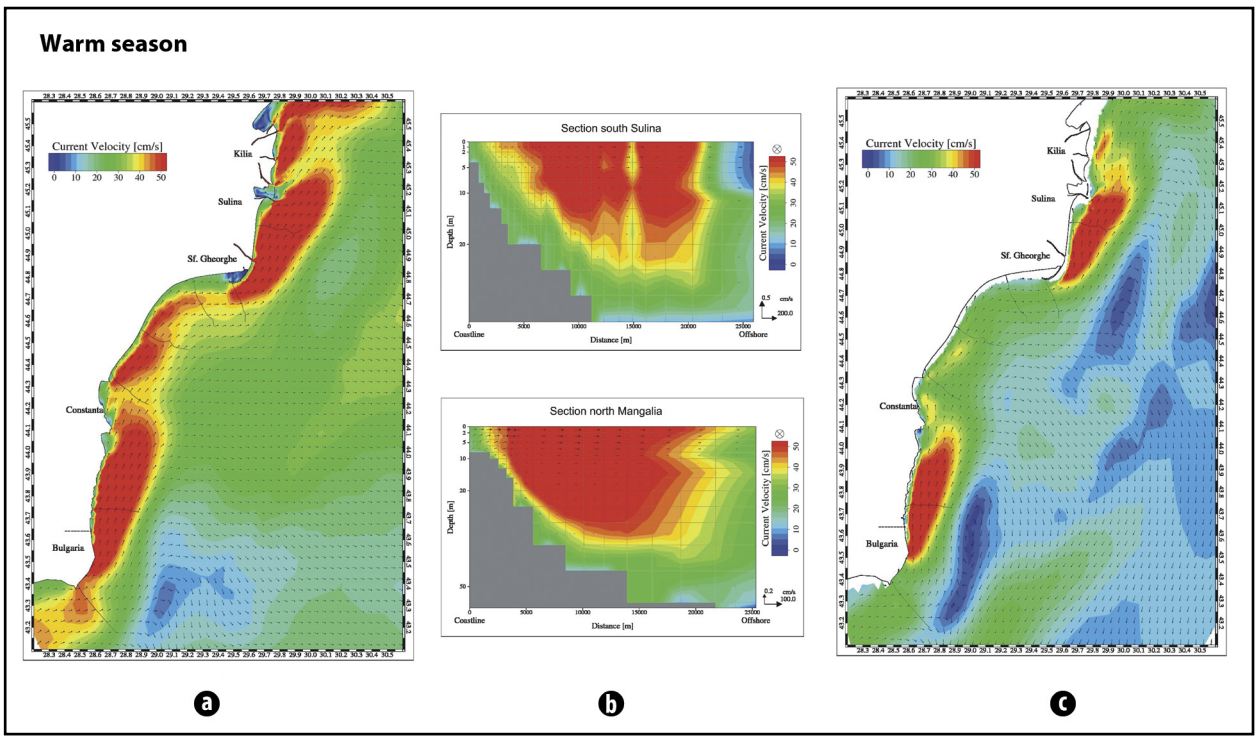

Fig 10. Current patterns along the Romanian Black Sea coast during the cold (upper panel) and warm seasons (lower panel): **a)** map of surficial currents; **b)** currents in the cross-sections located S of Sulina and N of Mangalia; **c)** map of currents at a depth of 9 m – wind from SW with 10 $m \cdot s^{-1}$, high Danube discharge.

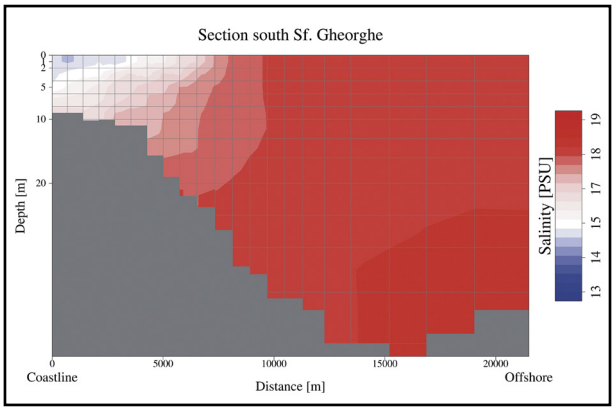

a) wind NE, 5 m/s, low Danube discharge

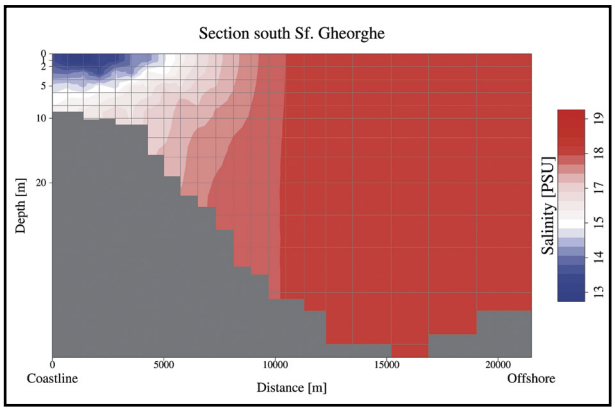

b) wind NE, 10 m/s, high Danube discharge

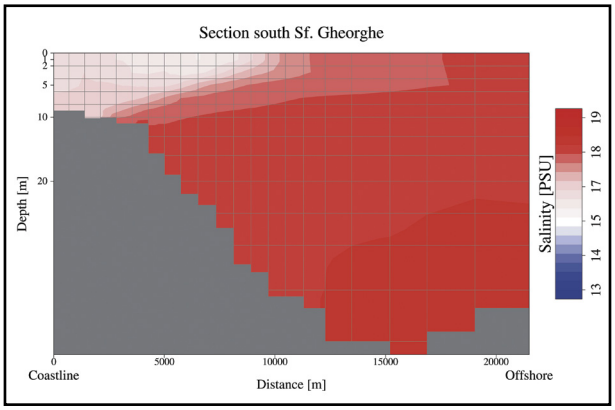

c) wind SE, 5 m/s, low Danube discharge

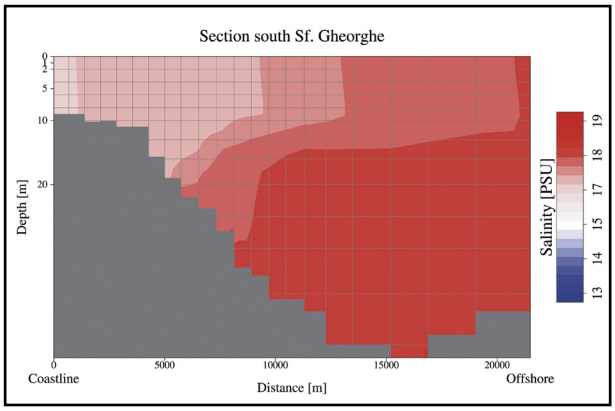

d) wind SE, 10 m/s, high Danube discharge

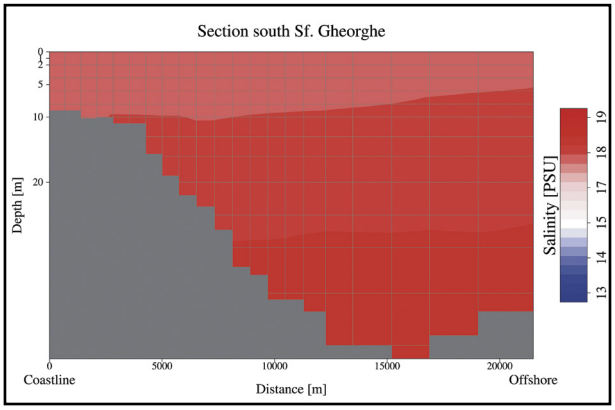

e) wind SW, 5 m/s, low Danube discharge

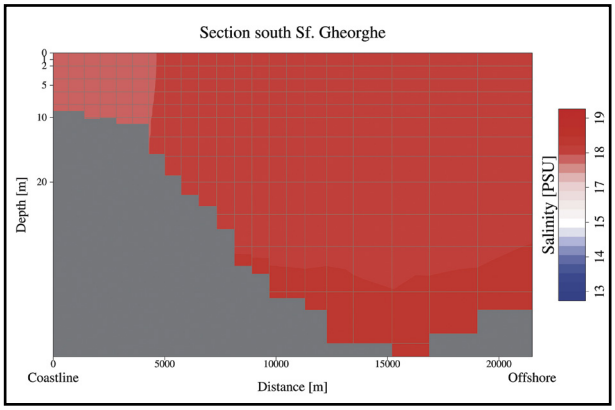

f) wind SW, 10 m/s, high Danube discharge

Fig 11. Salinity on the cross-section located S of Sf. Gheorghe in different conditions, cold season.

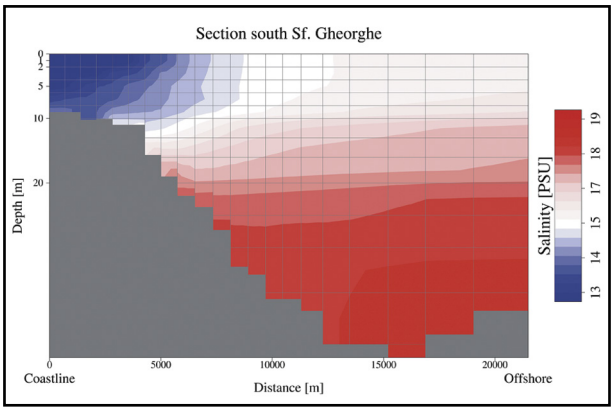

a) wind NE, 5 m/s, low Danube discharge

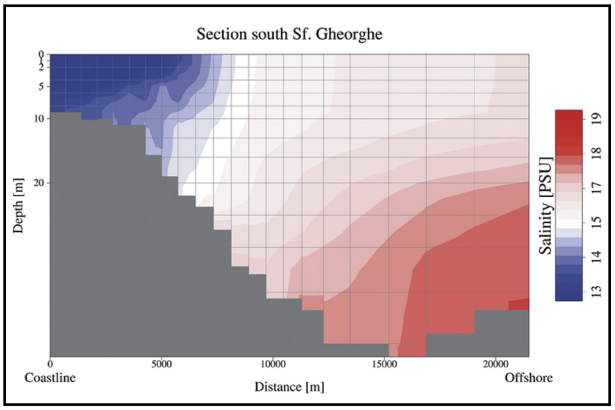

b) wind NE, 10 m/s, high Danube discharge

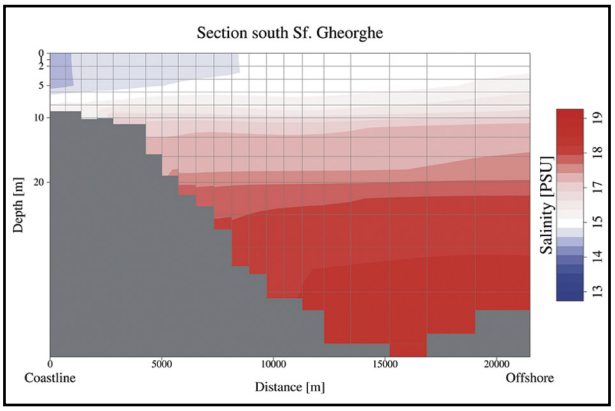

c) wind SE, 5 m/s, low Danube discharge

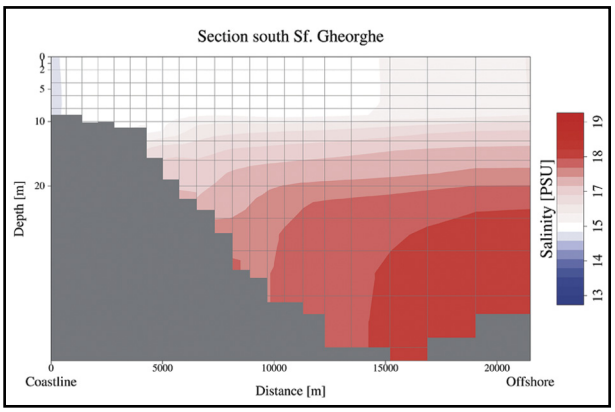

d) wind SE, 10 m/s, high Danube discharge

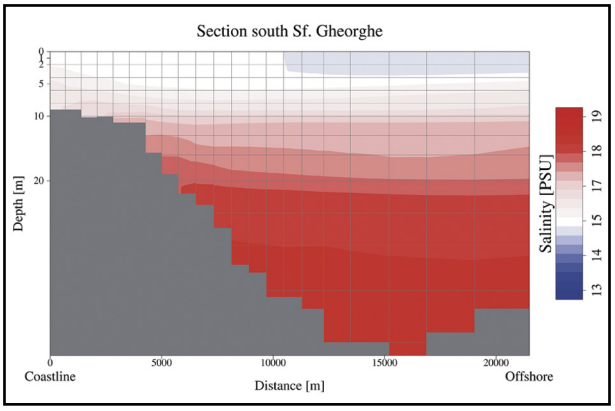

e) wind SW, 5 m/s, low Danube discharge

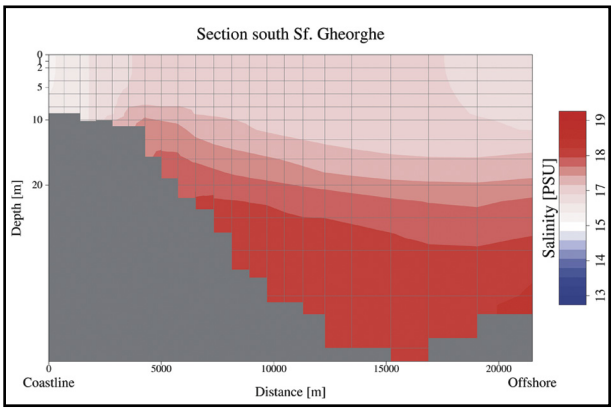

f) wind SW, 10 m/s, high Danube discharge

Fig 12. Salinity on the cross-section located S of Sf. Gheorghe in different conditions, warm season.

The ADCP profiles I to IX, between the Sulina and Sf. Gheorghe distributaries, were acquired on June 22, when the wind was blowing from south, with a speed of 5.4 m·s^{-1}. On the previous day, the wind also blew from south, with a speed of 3 m·s^{-1}, a condition that can be considered almost as calm during the warm season. The surface current directions on the ADCP profiles I to VI (Fig. 13), located at south of the Sulina jetty, show S to N components. These current pathways can also be noticed on the model map of the surface currents, in calm conditions and for the beginning of the warm season. For the ADCP profiles V and VI (Fig. 13), the surface current directions suggest the presence of the eddy-like current occurring between the Sulina and Sf. Gheorghe distributaries, which is emphasized by the simulations in calm conditions (Fig. 5), with its stronger northern component, while just near the shoreline, the current direction is southward. Velocities between 20 and 30 cm·s^{-1} were measured. These values agree with the magnitude of the simulated currents from the first layer of the model (Fig. 13). The profiles VII to IX show southward velocity components close to the shore, higher than 20 cm·s^{-1}, which do not agree with the simulated currents in the first layer of the model.

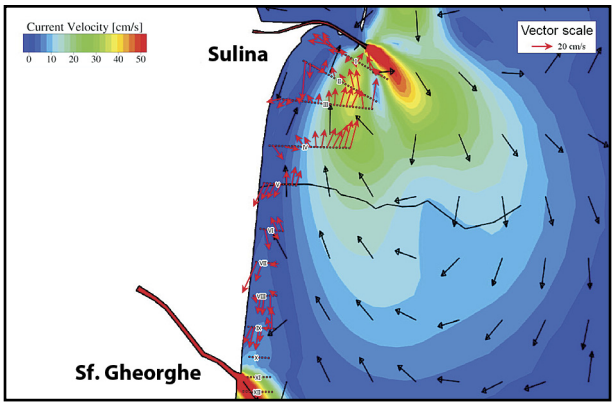

Fig 13. Current velocity and direction provided by ADCP *vs*. model results south of the Sulina distributary – calm conditions, medium Danube discharge, warm season.

The profiles X and XI, north of the Sf. Gheorghe mouth, and the profiles XII to XV, between the Sf. Gheorghe mouth and the southern end of the Sahalin spit, were acquired on June 18, when the wind was blowing from SE with a speed of 4.2 m·s^{-1}. The current field is represented on the map provided by the model, forced by a wind from south with a speed of 5 m·s^{-1}. The profiles X to XII show strong northward components (Fig. 14). The profiles XIII and XIV do not agree with the simulated currents from the first layer of the model, but the profile XV provides a slightly better fit.

The ADCP transects XVI and XVII were acquired on June 19, when the wind was blowing from S, at 8.3 m·s^{-1}, according to the available information. However, we think that it would have been exaggerated to setup a simulation with constant wind speed around 8 m·s^{-1}, as we have no information if this lasted during that day. Therefore, the resulting surface current directions were represented on the current map with the wind forcing of 5 m·s^{-1} instead (Fig. 14). This is the reason why the measured current velocities, that exceed 30 cm·s^{-1}, are higher than the simulated values, which are around 25 – 30 cm·s^{-1}.

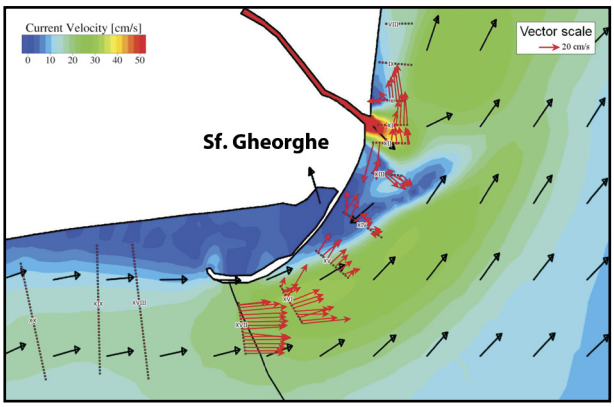

Fig 14. Current velocity and direction provided by ADCP *vs*. model results in the zone of the Sf. Gheorghe distributary – wind from S with 5 m·s^{-1}, medium Danube discharge, warm season.

The ADCP profiles XXVII to XXXIV, located along the Sinoe lagoon, were acquired on May 21, on almost calm conditions (wind from north at 3 m·s^{-1}). On the previous day, the wind was also from north, with a speed of 5.2 m·s^{-1}. We can thus compare the distribution of the surface current to the pattern provided by the simulation forced by a wind from north at 5 m·s^{-1} (Fig. 15). The measured current directions obviously correspond to those given by the model. However, while the simulated current velocity at a depth of 1 m is around 25 cm·s^{-1}, the experimental data locally exceed 30 – 40 cm·s^{-1}, as seen on the ADCP profiles XXIX, XXXI, XXXIV. These differences may be due to an increased wind velocity that probably occurred a couple of hours before the measurements.

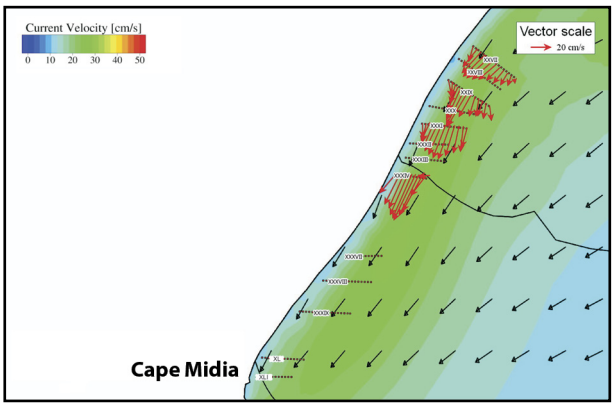

Fig 15. Current velocity and direction provided by ADCP *vs*. model results north of Cape Midia – wind from N with 5 m·s^{-1}, medium Danube discharge, warm season.

Differences between measured and simulated currents were expected at this stage of the study, because detailed information on the wind forcing and on the variation of the Danube discharge were not yet available, and also because

Table 3. Comparison of current velocity and direction - Historical data versus model results

Location	Wind	Historical data	Simulation results	
			cold season	*warm season*
Sulina – meteorological station	calm	~ 1 – 2 cm·s^{-1}; ENE – W	~ 2 cm·s^{-1}; eddy-like current; NE	2 cm·s^{-1}; eddy-like current; NE
	NE 5 m·s^{-1}	4 – 5 cm·s^{-1}; S – SW	~ 5 cm·s^{-1}; S – SW	~ 5 cm·s^{-1}; S – SW
	NE 10 m·s^{-1}	5 – 7 cm·s^{-1}; S – SW	7 – 10 cm·s^{-1}; SSW	7 – 10 cm·s^{-1}; SSW
	SE 5 m·s^{-1}	5 cm·s^{-1}; WNW	5 cm·s^{-1}; WNW velocity component	5 cm·s^{-1}; WNW velocity component
	SE 10 m·s^{-1}	6 – 12 cm·s^{-1}; WNW	8 – 10 cm·s^{-1}; WNW velocity component	10 – 12 cm·s^{-1}; WNW velocity component
	SW 5 m·s^{-1}	3 – 4 cm·s^{-1}; ENE	~ 5 cm·s^{-1}; ENE velocity component	~ 5 cm·s^{-1}; ENE velocity component
	SW 10 m·s^{-1}	5 – 11 cm·s^{-1}; ENE	10 cm·s^{-1}; ENE velocity component	15 cm·s^{-1}; ENE velocity component
Sulina – beach	calm	12 – 15 cm·s^{-1}; S for N-NE wind and NNE for S and E wind	12 – 15 cm·s^{-1}; eddy-like current; NNE	5 – 8 cm·s^{-1}; NNE (eddy-like current)
	NE 5 m·s^{-1}	~ 15.5 cm·s^{-1}; SSW	15 cm·s^{-1}; SSW	12 – 15 cm·s^{-1}; SSW
	NE 10 m·s^{-1}	~ 20 cm·s^{-1}; SSW	20 cm·s^{-1}; SSW	20 cm·s^{-1}; SSW
	SE 5 m·s^{-1}	18 cm·s^{-1}; NNE	~ 18 cm·s^{-1}; NNE	~ 10 cm·s^{-1}; NNE
	SE 10 m·s^{-1}	~ 20 cm·s^{-1}; NNE	18 – 20 cm·s^{-1}; NNE	~ 20 cm·s^{-1}; NNE
	SW 5 m·s^{-1}	17 cm·s^{-1}; NNE	15 – 17 cm·s^{-1}; NNE	15 cm·s^{-1}; NNE
	SW 10 m·s^{-1}	~ 20 cm·s^{-1}; NNE	20 cm·s^{-1}; NNE	~ 20 cm·s^{-1}; NNE
Sf. Gheorghe – beach	calm	13.3 – 16.7 cm·s^{-1}; S for wind from N-NE, W-NW; N for wind from S-SE	10 – 15 cm·s^{-1}; S – SSE	10 – 12 cm·s^{-1}; S
	NE 5 m·s^{-1}	22 cm·s^{-1}; S	20 cm·s^{-1}; S – SSE	20 cm·s^{-1}; S
	NE 10 m·s^{-1}	30 – 35 cm·s^{-1}; S	35 cm·s^{-1}; S	35 cm·s^{-1}; S
	SE 5 m·s^{-1}	20 – 28 cm·s^{-1}; N	15 cm·s^{-1}; N	15 cm·s^{-1}; N
	SE 10 m·s^{-1}	30 – 35 cm·s^{-1}; N	30 cm·s^{-1}; N	35 cm·s^{-1}; N
	SW 5 m·s^{-1}	22 – 25 cm·s^{-1}; N	25 cm·s^{-1}; N	15 cm·s^{-1}; N
	SW 10 m·s^{-1}	~ 30 cm·s^{-1}; N	30 cm·s^{-1}; N	30 – 35 cm·s^{-1}; N

the density currents are idealized. However, we consider this discussion an important step towards a better validation of modelling results.

A simulation with real wind forcing, real Danube discharge for the period of the measurements, as well as with the temperature and salinity fields for June is included in the future steps of the research work.

3.3. Simulated currents under various wind conditions

Even if the currents provided by the simulations are formed under the combined influence of wind, Danube discharge, distribution of temperature and salinity, we will attempt to discuss the influence of each of these factors.

3.3.1. Influence of wind

In the absence of wind, a longshore current occurs along the Romanian Black Sea coast (Fig. 4), due to the Danube buoyant flow. The model emphasizes the eddy-like currents, due to the discharge of the Danube distributaries and to the presence of the Sulina jetties, described in previous works, such as Panin (1998), Giosan *et al*. (1999), Tescari *et al*. (2006), Stănică and Panin (2009).

As a result of constantly-blowing wind, the eddy-like currents disappear. The wind determines the main direction of the surface current, especially at higher velocity (Figs. 5 – 10). The zone with high current velocities may reach a depth of 30 m, especially for the NE and SW wind direction, parallel to the coast, as shown on the cross-sections from Figs. 6, 9 and 10.

As analysed by Yankovsky *et al*. (2004), for the northwestern part of the Black Sea, northeasterly winds are downwelling-favourable, enhancing the predominantly cyclonic circulation, discussed by Poulain *et al*. (2005), while southwesterly winds are upwelling-favourable, being opposite to it. For the warm season and a low Danube river discharge the simulation roughly approaches the situation of July 1992, described in the work of Yankovsky *et al*. (2004), when the Danube buoyant flow penetrated all the way along the western coast of the Black Sea, favoured by northeasterly wind, occurring prior and during to the observation period. The total Danube discharge at that time was 3000 $m^3 \cdot s^{-1}$, lower than the minimum discharge in our analysis.

The wind from SE does not create strong currents, as it is perpendicular to the coast. It doesn't affect deeper layers, as shown on the current cross-sections reported in Figs. 7 and 8.

Wind from SW is opposite to the downdrift propagation of the Danube buoyant flow. With such a wind direction and the high Danube discharge conditions we expected the forcings to get closer to the situation discussed by Yankovsky *et al*. (2004), for May 1994, when buoyant flow was spread offshore and didn't reach Cape Kaliakra. The total Danube river discharge at that time was 11000 $m^3 \cdot s^{-1}$. This value is higher than the maximum discharge in our analysis.

Looking carefully at the cross-sections from the Figs. 5 and 6, for the NE wind, one can notice that the velocity vectors show a deepening trend, which suggests that downwelling occurs. Similarly, for the cross-sections from the Figs. 9 and 10, for the SW wind, the velocity vectors are upward and towards offshore, which suggests that upwelling occurs.

Thus, these observations are in agreement with the analysis carried out by Yankovsky *et al*. (2004).

3.3.2. Influence of temperature and salinity

As emphasized by the simulations performed in calm conditions, the longshore current occurring along the Romanian Black Sea coast is stronger during the cold season, as the freshwater density is higher, resulting in a higher buoyancy.

For the simulations with wind forcing, the stratification due to temperature distribution, thus due to the initial condition in our model, is stronger during the warm season and controls the efficiency of the wind-induced mixing, as discussed by Yankovsky *et al*. (2004). Therefore, under the same conditions of wind and discharge, current velocities may be higher than in the cold season, and this may also occur in deeper layers, as shown by the cross-sections of Figs. 6, 9 and 10. This occurs especially for the wind directions parallel to the coast, NE and SW.

Salinity was analysed on the cross-section located south of the Sf. Gheorghe distributary, for the simulations with wind forcing. This cross-section was chosen because it takes over a significant part of the Danube buoyant flow.

The salinity distributions, represented in Figs. 11 (for the cold season) and 12 (for the warm season), show as the Danube buoyant flow is pushed towards the coast with wind from NE, while with SW wind, it is forced offshore and undergoes a more intense mixing.

Downwelling-favourable northeasterly wind tends to deepen the buoyant layer, especially in the warm season, as mentioned by Yankovsky *et al*. (2004) in their analysis of the situation in July 1992. The higher the wind speed the deeper the buoyant flow moves, as shown by Figs.12a, b. The upwelling-favourable wind from SW blocks the downdrift propagation of the buoyant flow, especially in the warm season. At higher wind velocity, one can notice a slight increase of salinity in the upper layers (Figs. 12e, f). This can be regarded as an "upwelling effect".

With wind from SE, the salinity cross-sections show "an intermediate situation" with respect to the other wind forcings, so that the buoyant flow is less strongly forced offshore than in the case of SW wind, or is only weakly pushed towards the coast compared to the case of a wind from NE (Figs. 11c, d and 12c, d).

3.3.3. Fluxes

Calculated fluxes on the selected cross-sections from Fig. 3 reflect the combined influence of wind, Danube discharge and temperature and salinity.

The fluxes calculated on the selected cross-sections, for total Danube discharge values of 4000, 6500 and 9000 $m^3 \cdot s^{-1}$, show significant changes between the cold season and warm season, as described in a previous study by Dinu *et al*. (2011). These changes occur for various wind forcing and also in calm conditions.

In the absence of wind, the calculated northward fluxes on the cross-section located north of Mangalia, for all the three discharge magnitudes, are significant during the warm season: more than 20000 $m^3 \cdot s^{-1}$, as a low velocity eddy-like current can be found (Fig. 4). During the cold season, there is no northward flux on this cross-section, as the current direction is southward, parallel to the coast. For all the discharge magnitudes imposed in the simulations, the calculated southward fluxes are higher during the cold season, especially on the cross-sections located north of Mangalia (more than 100000 $m^3 \cdot s^{-1}$) and in Bulgaria (more than 200000 $m^3 \cdot s^{-1}$).

Northeasterly wind at 5 $m \cdot s^{-1}$ leads to higher southward fluxes during the cold season. In the cold season, the flux calculated for the cross-section in Bulgaria is over 300000 $m^3 \cdot s^{-1}$ and, in the warm season, it is less than 250000 $m^3 \cdot s^{-1}$. When the NE wind velocity is increased to 10 $m \cdot s^{-1}$, there is no significant difference between the calculated fluxes for the cold and warm seasons, in all the cross-sections.

The fluxes calculated for the wind velocity of 10 $m \cdot s^{-1}$ can be significantly higher than the ones for 5 $m \cdot s^{-1}$, both for the cold and warm seasons, for the three analyzed directions, as shown in Dinu *et al*. (2011). In the case of wind from NE with 10 $m \cdot s^{-1}$, both for the cold and warm seasons, the fluxes calculated for the cross-section in Bulgaria are around 600000 $m^3 \cdot s^{-1}$, twice than in the case of wind with 5 $m \cdot s^{-1}$.

The wind from SE leads to rather similar results on the southward fluxes calculated on the selected cross-sections. These are lower than for a wind from NE, as suggested by comparing the currents in the Figs. 5 and 7, for a wind velocity of 5 $m \cdot s^{-1}$, and Figs. 6 and 8, for a wind velocity of 10 $m \cdot s^{-1}$. Since the wind mainly affects the current directions in the uppermost layer, the southward fluxes are mostly driven by the general circulation, whose southward components are larger (Figs. 7 and 8). For a wind velocity of 10 $m \cdot s^{-1}$, the calculated flux for the cross-section in Bulgaria is less than 350000 $m^3 \cdot s^{-1}$.

The wind from SW leads to stronger currents and significantly higher northward fluxes during the warm season (Figs. 9 and 10), especially for the wind velocity of 10 $m \cdot s^{-1}$. Dinu *et al*. (2011) showed that, for an increased SW wind velocity, the calculated northward fluxes are almost the same, regardless of the Danube discharge. For a wind velocity of 10 $m \cdot s^{-1}$, the calculated flux on the cross-section located north of Mangalia is around 270000 $m^3 \cdot s^{-1}$, in the cold season, and around 420000 $m^3 \cdot s^{-1}$, in the warm season.

Moreover, for all the considered wind regimes, the calculated fluxes in all the cross-sections have similar magnitudes, regardless of the Danube discharge values used in the analysis.

Considering the results of the simulations for all the imposed forcings, we can infer that wind is a dominant factor controlling the current circulation, with a stronger influence than the distribution of temperature and salinity.

Even if the discussed simulations are theoretical, the model results can give a synthetic description of the observed pathways of the currents along the Romanian Black Sea coast and how these are affected by the main forcings, which are essentially the wind and the Danube river discharge. Based on the results of this analysis, the wind appears to be the most important factor in the evolution of the coastal currents in the studied area.

CONCLUSIONS

An analysis of the effects of wind and of the river Danube flow on the circulation along the Romanian Black Sea coast was performed, using the open-source 3D numerical model SHYFEM. Several simulations were carried out, varying the wind velocity and direction and the Danube river discharge. The results obtained in various wind conditions, with initial states for cold season and warm season, have been discussed in this study. The available historical data, as well as data from measurements carried out in 2011, are compared to the results provided by simulations with almost similar wind forcing and Danube river discharge. However, although no detailed data on the real forcing were used so far, the results discussed in this paper in the light of experimental data represent a first significant step towards a better validation of our model tools.

In our analysis we also considered the results of a previous study on the effects of the Danube buoyant flow on the NW part of the Black Sea. Even if the described situations are simplified compared to the analysis by Yankovsky *et al*. (2004), our simulations provide currents of the same order of magnitude and lead to similar observations concerning the influence of the Danube buoyant flow on the current intensities and pattern.

The model emphasizes that the longshore current that occurs along the northwestern Black Sea coast can be found even in the absence of wind, and that it is driven by the Danube river buoyant flow.

However, a constantly blowing wind becomes an important factor in the formation of coastal currents, both in the cold and warm seasons. The downwelling-favourable NE wind deepens the Danube buoyant layer, especially in the warm season. The upwelling-favourable wind from SW blocks the propagation of the Danube buoyant flow, espe-

cially in the cold season. These findings are in agreement with situations described in the previous study by Yankovsky *et al*., 2004. The northeasterly and southwesterly winds lead to stronger currents than the wind from SE, as they are parallel to the coastline.

According to the results of our investigations, the wind, in general, is the main factor controlling the overall coastal water circulation in the area considered.

Future modelling work will include simulations with real wind forcing from the period of the field campaign. This will permit a better validation of the theoretical model.

This study attempts to put together the available results of field and modelling works, which would lead to a better understanding of the coastal hydrodynamics.

The issues raised hereby could be of interest for the Romanian Black Sea coast scientists, since modelling hasn't been applied to study this area in detail.

ACKNOWLEDGEMENTS

This work was partly performed within the research project CLASS, contract 32-130/2008, funded by ANCS, the Romanian Authority for Scientific Research, and partly within the bilateral project nr. 639/2013. We thank Dr. Constantin Bondar from GeoEcoMar (Bucharest, Romania), for providing the historical wind and currents data on the Romanian Black Sea coast.

REFERENCES

Bajo M., Umgiesser G. (2010) – Storm surge forecast through a combination of dynamic and neural network models. *Ocean Modelling*, **33**, 1 – 9.

Beckers J. M., Grégoire M. L., Nihoul J.C.J.., Stanev E., Staneva J., Lancelot C. (2002) – Modelling the Danube-influenced northwestern continental shelf of the Black Sea. I: Hydrodynamical processes simulated by 3-D and box models. *Estuarine, Coastal and Shelf Science*, **54**, 453 – 472.

Bellafiore D., Umgiesser G., Cucco A. (2008) – Modeling the water exchanges between the Venice Lagoon and the Adriatic Sea. *Ocean Dynamics*, **58**, 397 – 413.

Bondar C., Roventa V., State I. (1973) – *The Black Sea in the zone of the Romanian coast. Hydrological monography* (in Romanian), IMH Bucharest, 1 – 516.

Bondar C., State I., Cernea D., Harabagiu E. (1991) – Water flow and sediment transport of the Danube at its outlet into the Black Sea. *Meteorology and Hydrology*, **21** (*1*), Bucharest, 21 – 25.

Bondar C., Panin N. (2001) – The Danube Delta hydrologic data base and modelling. *Geo-Eco-Marina*, **5**-**6**, Bucharest - Constanta, Romania, 5 – 52.

Bondar C. (2006) – Hydrological information concerning the tsunami phenomenon in the Black Sea, including the Romanian coast. *Natural Hazard: Tsunami Events in the Black Sea*. (in Romanian), Bucharest, 92 – 102.

Burchard H., Petersen O (1999) – Models of turbulence in the marine environmental comparative study of two equation turbulence models. *Journal of Marine Systems*, **21**, 29 – 53.

Dan S., Stive M., Van der Westhuysen A. (2007) – Alongshore sediment transport capacity computation on the coastal zone of the Danube Delta using a simulated wave climate. *Coastal Zone Processes and Management. Environmental Legislation. Geo-Eco-Marina*, **13**, 21 – 30.

Dan S., Stive M.J.F., Walstra D.J., Panin N. (2009) – Wave climate, coastal sediment budget and shoreline changes for the Danube Delta. *Marine Geology*, **262**, issues *1-4*, 39 – 49.

De Pascalis F., Umgiesser G., Alemanno S., Basset A. (2009) – Numerical model study in Alimini Lake (Apulia Italy). *Sedimentary Processes and Deposits within River-Sea Systems. Geo-Eco-Marina*, **15**, 21 – 28.

Dinu I., Bajo M., Umgiesser G., Stănică A. (2011) – Influence of wind and freshwater on the current circulation along the Romanian Black Sea coast. *Geo-Eco-Marina*, **17**, 13 – 26.

Ferrarin C., Umgiesser G. (2005) – Hydrodynamic modeling of a coastal lagoon: The Cabras lagoon in Sardinia, Italy. *Ecological Modelling*, **188**, 340 – 357.

Ferrarin C., Razinkovas A., Gulbinskas S., Umgiesser G., Bliūdžiutė L. (2008) – Hydraulic regime-based zonation scheme of the Curonian Lagoon. *Hydrobiologia*, **611**, 133 – 146.

Ghezzo M., Guerzoni S., Cucco A., Umgiesser G. (2010) – Changes in Venice Lagoon dynamics due to construction of mobile barriers. *Coastal Engineering*, **57** (*7*), 694 – 708.

Giosan L., Bokuniewicz H., Panin N., Postolache I. (1999) – Longshore Sediment Transport Pattern along the Romanian Danube Delta Coast. *Journal of Coastal Research*, **15** (*4*), 859 – 871.

Kara A.B., Wallcraft A.J., Hurlburt H. (2005) – A new solar radiation penetration scheme for use in ocean mixed layer studies: An application to the Black Sea using a fine-resolution Hybrid Coordinate Ocean Model (HYCOM). *Journal of Physical Oceanography*, **35**, 13 – 32.

Kara A.B., Wallcraft A.J., Hurlburt H., Stanev E.V. (2008) – Air-sea fluxes and river discharges in the Black Sea with a focus on the Danube and Bosphorus. *Journal of Marine Systems*, **74** (*1-2*), 74 – 95.

Oguz T., Malanotte-Rizzoli P. (1996) – Seasonal variability of wind and thermohaline driven circulation in the Black Sea: Modeling studies. *Journal of Geophysical Research*, **101**, 16551 – 16569.

Panin N. (1998) – *Danube Delta: Geology, Sedimentology, Evolution*. Association des Sédimentologistes Français, Paris, 65 p.

Panin N. (2003) - The Danube Delta. Geomorphology and Holocene Evolution: a Synthesis / Le delta du Danube. Géomorphologie et évolution holocène: une synthèse. In: *Géomorphologie: relief, processus, environnement*, **9** (*4*), Paris, 247 – 262.

Panin N. (2005) – The Black Sea coastal zone – an overview. *European Seas: Coastal Zones and Rivers – Sea System*. *Geo-Eco-Marina*, **11**, 21 – 40.

Panin N., Jipa D. (2002) – Danube River Sediment Input and its Interaction with the North-western Black Sea. *Estuarine, Coastal and Shelf Science*, **54**, *2*, Elsevier, UK, 551 – 562.

Poulain P.M., Barbanti R., Motyzhev S., Zatsepin A. (2005) – Statistical description of the Black Sea near-surface circulation using drifters in 1999 – 2003. *Deep-Sea Research* I, **52**, 2250 – 2274.

Smagorinsky J. (1963) – General circulation experiments with the primitive equations, I. The basic experiment. *Monthly Weather Review,* **91**, 99 – 152.

Smith S., Banke E. (1975) – Variation of the sea surface drag coefficient with wind speed. *Quart. J. Roy. Meteorol. Soc*. **101**, 665 – 673.

Spătaru A. N. (1990) – Breakwaters for the protection of Romanian beaches. *Coastal Engineering*, **14**, 129 – 146.

Stanev E.V., Beckers J.M. (1999a) – Barotropic and baroclinic oscillations in strongly stratified ocean basins. Numerical study for the Black Sea. *Journal of Marine Systems*, **19** (*1-3*), 65 – 112.

Stanev E.V., Beckers J.M. (1999b) – Numerical simulations of seasonal and interannual variability of the Black Sea thermohaline circulation. *Journal of Marine Systems*, **22**, 241 – 267.

Stanev E.V., Bowman M.J., Peneva E. L., Staneva J.V. (2003) – Control of Black Sea intermediate water mass formation by dynamics and topography: Comparisons of numerical simulations, survey and satellite data. *Journal of Marine Research*, **61**, 59 – 99.

Staneva J.V., Dietrich D.E., Stanev E.V., Bowman M.J. (2001) – Rim current and coastal eddy mechanisms in an-eddy resolving Black Sea general circulation model. *Journal of Marine Systems*, **31**, 137 – 157.

Stanev E.V. (2005) – Understanding Black Sea dynamics. An overview of recent numerical modelling. *Oceanography*, **18** (2), p. 56 – 75.

Stănică A., Dan S., Ungureanu G. (2007) – Coastal changes at the Sulina mouth of the Danube River as a result of human activities. *Marine Pollution Bulletin*, **55**, 555 – 563.

Stănică A., Panin N. (2009) – Present evolution and future predictions for the deltaic coastal zone between the Sulina and Sf. Gheorghe Danube river mouths (Romania). *Geomorphology*, **107**, 41 – 46.

Stănică A., Dan S., Jiménez J.A., Ungureanu G.V. (2011) – Dealing with erosion along the Danube Delta coast. The CONSCIENCE experience towards a sustainable coastline management. *Ocean & Coastal Management,* **54**, 898 – 906.

Tescari S., Umgiesser G., Ferrarin C., Stănică A. (2006) – Current circulation and sediment transport in the coastal zone in front of the Danube Delta. *Coastal Zones and Deltas*, *Geo-Eco-Marina*, **12**, 5 – 16.

Umgiesser G., Melaku Canu D., Cucco A., Solidoro C. (2004) – A finite element model for the Venice Lagoon. Development, set up, calibration and validation. *Journal of Marine Systems*, **51**, 123 – 145.

Ungureanu G., Stănică A. (2000) – Impact of human activities on the evolution of the Romanian Black Sea beaches. *Lakes & Reservoirs: Research and Management*, **5**, 111 – 115.

Vespremeanu-Stroe A., Constantinescu Ş., Tătui F., Giosan L. (2007) – Multidecadal Evolution and North Atlantic Oscillation Influences on the Dynamics of the Danube Delta shoreline. *Journal of Coastal Research*, SI **50** (*Proceedings of the 9th International Coastal Symposium*), 157 – 162.

Yankovsky A.E., Lemeshko E. M., Ilyin Y. P. (2004) – The influence of shelf-break forcing on the alongshelf penetration of the Danube buoyant water, Black Sea. *Continental Shelf Research*, **24**, 1083 – 1098.